PHILOSOPHICAL TRANSACTIONS OF THE ROYAL SOCIETY A MATHEMATICAL, PHYSICAL & ENGINEERING SCIENCES

The Analysis of Geomagnetic Storm-Time Variations

R. J. Jady and R. T. Marshall

Phil. Trans. R. Soc. Lond. A 1984 **310**, 365-406
doi: 10.1098/rsta.1984.0001

Phil. Trans. R. Soc. Lond. A **310**, 365–406 (1984) [365]
Printed in Great Britain

THE ANALYSIS OF GEOMAGNETIC STORM-TIME VARIATIONS

BY R. J. JADY AND R. T. MARSHALL†
Department of Mathematics, The University of Exeter, Exeter EX4 4QE, U.K.

(*Communicated by S. K. Runcorn, F.R.S. – Received 7 June* 1982)

CONTENTS

One of the geomagnetic variation fields that has particular relevance to the problem of determining the global distribution of electrical conductivity in the upper mantle is the magnetic storm-time variation field, Dst. A mathematical description of such a naturally occurring phenomenon is therefore of importance. Major early contributions to the theory and analysis of magnetic storms were made by Chapman (1918), and later Chapman & Price (1930). With the advantage of modern computing facilities and techniques, and the availability of digitized data from an improved distribution of magnetic observatories, which resulted from the International Geophysical Year 1958, it is now possible to analyse such events for a greatly extended period, up to 10 days or so, after the storm onset. A set of 6 storms are analysed here, two of them occurred during the quiet part of the solar cycle (June 1964, and April 1965), and the remainder during a more active part (February 1969 (2 storms), March 1970, and August 1970). Data at hourly intervals, from at least 58 observatories within $\pm 55°$ latitude of the geomagnetic equator, were used for each storm. Values of

† Now at The British Petroleum Company, Britannic House, Moor Lane, London EC2Y 9BU, U.K.

the external and internal parts of the variation field have been obtained, and are given together with their associated errors for the dominant P_1 harmonic. An assessment of the results, based on statistical arguments, is also given.

1. Introduction

Geomagnetic storms have been of interest to geophysicists from the time before the early work of Birkeland (1908) to the present day. An outline of the theory and analysis of the storm-time variations, Dst, was given in two papers by Chapman (1918*a*, *b*). He took the average of several storms and by smoothing out local effects showed that the morphology of a typical storm has two main stages of development.

The initial, or main phase, is highly energetic and lasts for a few hours. During the main phase the horizontal component, H, of the magnetic field at first increases, but is followed by a significantly larger decrease. For the second, or recovery phase, the horizontal component gradually recovers to its pre-storm state. Corresponding changes in the vertical field component, Z, also occur. The overall duration of a single storm varies in individual cases from a few days to two weeks or so, though occasionally storms overlap and the period of geomagnetic disturbance is extended. Chapman concluded that the variation field consists of a primary part, associated with electric currents flowing outside the Earth, and a secondary part of internal origin. Comprehensive reviews of all aspects of the subject, and its historical development, can be found in Campbell & Matsushita (1967).

Chapman & Price (1930) analysed, into external and internal parts, the Dst field averaged over a group of storms. It was assumed that the field is axially symmetric and was therefore expressed in terms of the zonal harmonics $P_n(\cos\theta)$, where θ is the co-latitude, and n took the values 1, 3, 5. It was found that, with the exception of the first 10 h of the storm, the field can be adequately represented by the first harmonic P_1 alone. Modern computing facilities and numerical techniques, together with the availability of digitized data from an improved distribution of magnetic observatories, which resulted from the International Geophysical Year 1958, enable these conclusions to be statistically tested and amplified where appropriate.

Subsequent Dst analyses have been made. Rikitake & Sato (1957) analysed, at 4 hourly intervals, the Dst field for the first 32 h after the commencement of the storm of 18–19 June 1936. Data from 20 observatories were used. This particular storm differs somewhat in development from that of the group analysed by Chapman & Price (1930). The initial phase lasts about 12 h after the commencement, and the range in magnitude of the field values is much greater.

The 1936 storm data was re-examined by Anderssen & Seneta (1969). Their contribution was significant because of the statistical techniques that they developed to improve the estimates of the probable errors. They found that the total field was virtually the same as that determined by Rikitake & Sato (1957). However, 24 h after the beginning, the internal field was enhanced and the external field depressed compared with the earlier results.

Anderssen *et al.* (1970) assembled data from 51 observatories and analysed the first 36 h, at hourly intervals, of the storm commencing 25 September 1958. Unbiased estimators of the external and internal Dst fields were derived, and it was found that for this storm, the internal field is smaller overall, compared with the external field, than for the others. A discussion of the compatability of these analyses has been given by Jady *et al.* (1979). The storms analysed later in this paper have also been compared extensively and the details can be found in Marshall (1980).

The analysis of storm-time variations is important for the purpose of modelling the electrical conductivity distribution in the mantle on a global scale. The greater period of these variations, as compared to the daily variation, means that the induced currents penetrate further into the mantle. With Dst variations we therefore have penetration depths ranging from near-surface values, to 1000 km or so into the mantle. At these greater depths the induced currents are less influenced by near-surface lateral variations in conductivity. Information about the behaviour of the conductivity and the temperature profiles, particularly in those regions where phase changes in mantle materials occurs, is gained.

Inversion methods used in conductivity modelling (see, for example, Bailey (1970), Weidelt (1972), Parker (1972, 1977, 1980), Parker & Whaler (1981)) are mainly formulated for the case when the variation fields are expressed as functions of frequency rather than time. Analyses of Dst in the frequency domain have been made by Schmucker (1970, 1977), and Devane (1977). However, in the work presented here, storms are analysed in the time domain, and there are various important advantages in doing this.

First, each storm is analysed at discrete time steps, so that discontinuous records may be used. Stations previously discarded from frequency domain analysis can be included, thereby allowing a greater number of sites to be used. Second, it can be argued that methods of studying transient phenomena, such as Dst variations, are generally best formulated in the time domain. This is because Fourier transformation of the data is then unnecessary, and so the loss in resolution, which is inevitable with the use of a limited data window, is avoided.

Finally, a point that is often overlooked is that by working in the time domain, useful information concerning the morphology of the external and internal variation fields is readily available. It is therefore possible to visually check the compatibility of each site record to the overall representation of the field variations.

2. The nature of Dst

The physical mechanism of the storm-time variation field is fairly well understood. During a magnetic storm the Earth's main magnetic field, which can be realistically approximated by a geocentric dipole field, is influenced by changes in the pressure on the magnetosphere, of the solar wind plasma. On the sunward side of the Earth, the solar plasma compresses the magnetic field until the magnetic pressure within the magnetosphere balances the kinetic pressure of the solar wind.

At times of increased solar activity, the solar wind rapidly increases in energy density and causes both the distortion of the magnetosphere, and the injection into it of high energy particles. The sudden storm commencement, s.s.c., associated with this burst of energy, affects the magnetic field almost simultaneously (to within a few minutes) over the whole surface of the Earth. The initial increase in the horizontal field component is due to the compression of the magnetosphere, and the subsequent decrease is due to the enhancement of the ring current produced by the azimuthal drift of particles trapped within the magnetosphere. The gradual recovery to pre-storm conditions is caused by the loss of excess trapped particles from the ring current.

The symmetry of the system suggests that since Dst variations are mainly due to the ring current, the variations can be expressed in a series of Legendre polynomials, P_n, where n is odd. In practice this representation is not so useful for data obtained at high latitude sites. The Dst variations are distributed fairly uniformly over middle and low latitudes, but at latitudes greater

PHILOSOPHICAL TRANSACTIONS OF THE ROYAL SOCIETY A MATHEMATICAL, PHYSICAL & ENGINEERING SCIENCES

than about 55° they increase irregularly, probably because of intense currents flowing in the ionosphere around the auroral zones (Rikitake 1966).

Superimposed on the Dst variations there may also be magnetic bays and substorms, both lasting for periods of about a few hours (Matsushita 1964). Additionally, the solar daily variation is always present in records taken during magnetic storms. The daily variation, which has its maximum amplitude at local noon, is largely produced by two current vortices at a height of about 100 km in the ionosphere. The positions of the foci, one in the northern and one in the southern hemisphere, vary somewhat both during the day and during the year. The daily variation depends on local time, and is best represented as a series of associated Legendre polynomials P_n^m, whereas Dst depends on Universal Time, it must therefore be removed from the data before the Dst field is analysed.

It is possible that the Dst field contains a component with a daily period that is a function of latitude and U.T. It arises because the geomagnetic axis does not coincide with the geographic axis and so, as the Earth spins, the geomagnetic dipole moves relative to the plane of the ecliptic, and varies its latitude during the day to the solar wind. The component is likely to be small.

3. Data acquisition and preparation

3.1. *Storms analysed*

A set of six storms are analysed here. Two of them occur during the quiet part of the solar cycle. They begin at 18 h 52 min on 7 June 1964, and 13 h 13 min 17 April 1965 U.T. (*I.A.G.A. Bulletins* no. 12s2 1964, and no. 12t2 1965). The other four storms occur during the active part of the solar cycle. Their commencements are listed as (*I.A.G.A. Bulletins* no. 12x2 1969, and no. 32 a 1970), 15 h 2 min 2 February 1969, 20 h 24 min 10 February 1969, 14 h 17 min 8 March 1970, and 22 h 4 min 16 August 1970 (U.T.). There are clear differences in the results for quiet and active parts of the solar cycle, and these differences are discussed in § 5.

3.2. *Preliminary data preparation*

All data used in the analyses were expressed in Universal (World) Time, each hourly value being the mean value for that hour, centred on the half hour. It consisted, in the majority of cases, of declination D, horizontal H, and downward vertical Z field components for each site, though a few site records were of North X, East Y, and Z field components. The data describing the disturbances of June 1964 and April 1965 were obtained from the Institute of Geological Sciences (I.G.S.) at Edinburgh. It was recorded on magnetic tape in the standard digitized format as described in Report 16 (1975) of the Geomagnetism Unit of the I.G.S. Geophysical Division. A small part of the data used to analyse the February 1969, March 1970, and August 1970 disturbances was also supplied by I.G.S. However, the majority of the data for the 1969 and 1970 storms was obtained from World Data Centre A, and this was only available in the form of photocopies of tables taken from the observatory reports. The initial data preparation consisted of converting all records to U.T., followed by punching onto cards to be read into the computer for processing onto magnetic tape. Care was taken to match the format of these records to that of the I.G.S. data.

Before any analysis was attempted every site data sequence, each of 480 h duration, was plotted, together with an estimate of the associated power spectrum. These plots were checked for possible errors in data copying, and any seemingly unreliable records inspected in greater

detail. For example, there were a few cases of a change in baseline during the sequence that were not recorded correctly. It is felt that such a visual inspection of the data is of great importance and is strongly recommended. Finally, the field values for each site were transformed to X, Y, and Z field components where necessary.

The spherical harmonic analysis of Dst, in this study, is oriented to the geomagnetic centred dipole, the north pole of which was taken to be situated at co-latitude 11.5° and longitude 69° W. The geomagnetic coordinates of each site were calculated with the formulae given by Chapman & Bartels (1940, p. 646). These equations were also used to evaluate the angle ψ, subtended at each observatory by the great circles from the observatory to the geographic and geomagnetic north poles. X and Y were then transformed, by using the ψ value for each site, such that they were oriented to the geomagnetic centred dipole. Table 1 shows the geographic and geomagnetic coordinates of the sites used, together with the associated values of ψ.

After transforming the data to its required orientation, two fundamental problems remain: (i) to estimate and remove periodic variations, not associated with Dst, for each site data sequence, and (ii) to calculate and remove a realistic estimate of the baseline value for each observatory record.

In terms of amplitude, within the data sequences studied, by far the most important period variation, not associated with Dst, is that due to the daily variation S. Other periodic variations exist, for example the lunar variations (Malin 1973). These variations are significantly smaller than those due to S, of the order of a few nanoteslas, and are neglected here.

3.3. *Removal of daily variation*

Various methods of removing estimates of S from observatory data are available. One method is simply to leave the data as it stands and argue that, since a large number of sites is used, the effects will average out in the analysis. This simplistic approach has two main weaknesses. First, the observatories tend to be concentrated in certain areas of the globe, for example, in central Europe, see figure 1, and so S is not completely removed. Second, the error bars associated with the estimates of the field values are larger than necessary.

A further approach is to remove S with a moving average estimate throughout the sequence. This method also has two important failings. First, it affects the trend of a site data sequence in an unknown manner; some correction for this can be made (Anderssen & Seneta 1971), but the analysis is significantly complicated. Second, there is reason to believe that for several days following the s.s.c., there may exist a daily variation associated with Dst (see §2). A moving average approach would suppress this part of the periodic variation that belongs to Dst.

The method finally adopted for this study uses a least squares finite Fourier series representation of S. For each storm analysed, certain days of the 20 day data sequence, which did not contain the s.s.c. and the recovery phase were noted. On average this meant that at least 6 of the 20 days in a sequence were not used to estimate S because they were too disturbed. If any field value, at a given site, was missing then the day to which it belonged was also removed from the sequence used to estimate S for that site. Hence, if an observatory record did not contain at least a minimum number of unbroken quiet days the observatory record was removed from the storm analysis.

3.4. *Baseline estimation*

The problem of calculating a reliable objective estimate of the normal field baseline value was surprisingly difficult. The baseline may be regarded as the undisturbed field value, taken to be constant in terms of the timescales dealt with here.

PHILOSOPHICAL TRANSACTIONS OF THE ROYAL SOCIETY A MATHEMATICAL, PHYSICAL & ENGINEERING SCIENCES

TABLE 1. OBSERVATORIES USED AND THEIR COORDINATES

site	code	geographical position lat./deg	geographical position long./deg	geomagnetic position lat./deg	geomagnetic position long./deg	ψ	data availability 1964 X	1964 Z	1965 X	1965 Z	1969 X	1969 Z	1970a X	1970a Z	1970b X	1970b Z
lis Ababa	AA	9.03	38.77	5.4	109.2	−10.99	×	×	×	×		×	×	×	×	×
ıeria	AE	36.85	357.53	40.6	75.3	−13.94	×	×	×	×			×	×	×	×
khabad	AK	37.95	58.10	30.5	133.1	−10.64	×	×	×	×	×	×	×	×		
ɔag	AL	18.63	72.87	9.5	143.6	−7.17	×		×	×	×	×	×		×	×
berly	AM	−43.15	172.72	−47.7	252.5	15.11	×	×								
ıamalainagar	ANN	11.40	79.68	1.5	149.4	−5.95			×	×	×	×	×	×	×	
a	AP	−13.80	188.22	−16.1	260.2	11.67	×	×	×	×						
uila	AQ	42.38	13.32	42.9	92.9	−15.64	×	×	×	×	×	×	×	×	×	×
quipa	ARE	−16.47	288.52	−5.0	357.6	0.50	×									
gui	BA	4.43	18.57	4.8	88.5	−11.53	×	×	×	×				×		
lder	BD	40.13	254.77	49.0	316.5	10.34					×	×	×	×	×	×
k	BE	51.83	20.80	50.4	104.0	−18.24					×	×	×	×	×	×
kov	BV	49.07	14.02	49.1	96.4	−17.60					×	×	×	×	×	×
mbra	CI	40.22	351.58	45.0	70.2	−14.23	×	×	×	×	×	×			×	×
tle Rock	CR	37.23	237.87	43.5	298.6	12.70									×	×
ırbes	DB	50.10	4.60	52.0	87.7	−18.09	×	×	×	×	×	×	×	×	×	×
las	DS	32.98	263.25	43.0	327.7	7.29	×	×	×	×	×	×	×	×	×	×
uene	FQ	5.47	286.27	16.9	355.1	0.98	×		×	×		×	×	×	×	×
dericksburg	FR	38.20	282.63	49.6	349.8	2.56	×	×	×	×	×	×	×	×	×	×
ɛtown	FT	8.46	346.79	14.8	57.8	−9.82	×	×								
stenfeld Bruck	FU	48.17	11.28	48.8	93.3	−17.36			×	×	×	×	×	×	×	×
ıagara	GN	−31.78	115.95	−43.2	185.8	1.35	×	×	×	×	×	×	×	×	×	×
ım	GU	13.58	144.87	4.0	212.9	6.39	×		×	×		×	×	×	×	×
tland	HA	50.98	355.52	54.6	79.0	−18.11	×	×	×	×	×	×	×	×	×	×
banovo	HB	47.87	18.18	47.2	99.8	−17.03	×	×	×	×	×	×	×	×		×
ıolulu	HO	21.32	202.00	21.1	266.5	12.33	×	×	×	×	×	×	×	×	×	×
manus	HR	−34.42	19.23	−33.3	80.5	13.79	×	×	×	×	×	×	×	×	×	×
ıncayo	HU	−12.05	284.57	−0.6	353.7	1.28	×		×	×						
vana	HV	22.97	277.85	34.1	345.3	3.14			×	×						
derabad	HYD	17.42	78.55	7.6	148.9	−6.20			×	×	×	×	×	×	×	×
dan	IBN	7.43	3.90	10.7	74.7	−11.18					×				×	×
ıtsk	IR	52.17	104.45	40.7	174.7	−1.72					×	×	×	×	×	×
ıtsk	PY	52.17	104.45	40.7	174.7	−1.72				×						
ɛioka	KA	36.23	140.18	26.0	206.0	6.21	×	×	×	×	×					
nbul	KAN	41.07	29.07	38.5	107.5	−14.61					×	×		×		×
ɛan	KN	55.83	48.85	49.3	130.4	−15.69	×	×	×	×						
ɛan	KZN	55.83	48.85	49.3	130.4	−15.69					×	×				
laikanal	KOD	10.23	77.47	0.6	147.1	−6.32							×	×	×	×
ɔr	KR	7.33	134.50	−3.2	203.3	4.57	×	×		×						
v	KV	50.72	30.30	47.6	112.2	−16.96	×	×	×	×	×	×				
ıoya	KY	31.42	130.88	20.5	198.1	4.15	×	×	×	×	×	×	×	×	×	×
ıozan	KZ	35.25	139.97	25.0	205.9	6.12					×	×	×	×	×	×
ɛrono	LG	42.45	357.50	46.1	77.2	−15.28	×	×	×	×					×	×
ıping	LP	25.00	121.17	13.7	189.5	2.08						×	×	×	×	×
Quiaca	LQ	−22.10	294.40	−10.6	3.2	−0.69	×				×	×	×	×	×	×
ɛro	LW	−2.25	28.80	−3.8	97.2	−11.42	×	×	×	×			×			
v	LV	49.90	23.75	48.0	105.9	−17.32	×	×	×	×	×	×	×	×	×	×
ında	LU	−8.92	13.17	−7.2	80.6	−11.48	×	×	×						×	×
ɔour	MB	14.40	343.02	21.3	55.0	−9.71	×	×	×	×			×	×	×	×
ca	MC	3.35	8.67	5.7	78.6	−11.29	×	×	×	×			×	×	×	×
ɛuawa	MIZ	39.02	141.83	28.9	207.1	6.71							×		×	
allat	ML	29.52	30.90	26.9	105.9	−12.73	×	×	×	×	×	×		×	×	×
ısk	MN	54.50	27.88	51.6	111.8	−18.59	×	×	×	×	×		×	×	×	×
scow	MO	55.48	37.32	50.9	120.5	−17.65	×	×	×	×	×	×	×	×	×	
mambetsu	MT	43.90	144.20	34.0	208.4	7.57	×	×	×	×	×	×	×	×	×	×
ntinlupa	MU	14.37	121.02	3.0	189.7	1.99	×	×	×	×	×	×	×	×	×	×
megk	NI	52.07	12.68	52.2	96.6	−18.80	×	×	×	×	×	×	×	×	×	×
robi	NR	−1.28	36.83	−4.4	105.3	−11.09			×	×	×	×	×	×	×	×
ɛssa	OD	46.78	30.88	43.7	111.1	−15.76					×	×	×	×		
amaribo	PA	5.82	304.78	17.0	14.3	−2.85	×	×	×	×	×	×				
r	PI	−31.67	296.12	−20.2	4.6	−1.09	×				×	×	×	×	×	×
t Moresby	PM	−9.40	147.15	−18.6	217.9	7.13	×	×	×	×	×	×	×	×	×	×
agyurishte	PN	42.52	24.18	40.9	103.4	−15.26	×	×	×	×	×	×	×	×	×	

TABLE 1 (*cont.*)

site	code	geographical position lat./deg	geographical position long./deg	geomagnetic position lat./deg	geomagnetic position long./deg	ψ	data availability 1964 X	1964 Z	1965 X	1965 Z	1969 X	1969 Z	1970a X	1970a Z	1970b X	1970b Z
nice	PR	49.98	14.55	49.9	97.3	−17.91	×				×	×	×	×	×	×
rent	RO	44.30	7.88	45.8	88.4	−16.17			×	×	×	×	×	×	×	×
wala	SAB	30.33	77.80	20.5	149.7	−6.67					×	×				
ernando	SF	36.47	353.80	41.0	71.3	−13.58	×						×	×	×	×
uan	SJ	18.38	293.89	29.9	3.2	−0.66	×	×	×	×	×	×	×	×	×	×
ato	SS	33.57	135.93	23.0	202.4	5.24	×	×	×	×		×	×		×	×
	SSH	31.10	121.18	19.8	189.3	2.15							×	×	×	×
i	SU	44.68	26.25	42.5	106.1	−15.63	×	×	×	×	×	×	×	×	×	×
r	SW	52.12	21.25	50.6	104.6	−18.31	×	×	×	×						
nrasset	TA	22.80	5.53	25.4	79.6	−12.28							×	×	×	×
erang	TAG	−6.17	106.63	−17.6	175.4	−0.91					×	×			×	×
erang	TG	−6.17	106.63	−17.6	175.4	−0.91		×	×	×						
i	TAH	−17.55	210.38	−15.3	282.7	11.77								×	×	×
i	TB	42.08	44.70	36.7	122.1	−13.16	×	×	×	×			×	×	×	×
yucan	TE	19.75	260.82	29.6	327.0	6.62			×	×						
n	TEH	35.73	51.38	29.4	126.5	−11.38										×
ife	TEN	28.48	343.72	35.0	58.6	−11.16							×	×	×	×
o	TL	39.88	355.95	43.9	74.7	−14.51		×	×	×			×	×	×	×
narive	TN	−18.92	47.55	−23.7	112.5	−11.23	×	×	×	×	×	×		×	×	×
ngi	TO	−37.53	145.47	−46.7	220.8	9.46	×	×	×	×	×	×	×	×		
eb	TS	−19.22	17.70	−18.2	82.8	−12.09			×	×	×	×				
ca	TT	−1.20	311.48	9.6	20.8	−4.06			×	×						
n	TU	32.25	249.17	40.4	312.2	10.06	×	×	×	×	×	×	×	×	×	×
ndrum	TV	8.48	76.95	−1.1	146.4	−6.41	×	×	×		×		×	×	×	×
w	TW	−43.25	294.68	−31.8	3.2	−0.86			×	×	×	×				
y	TY	46.90	17.90	46.3	99.1	−16.74	×	×			×	×	×	×	×	×
Bator	ULB	47.85	106.75	36.4	176.5	−1.05						×				
uras	VA	−22.40	316.35	−11.9	23.9	−5.01					×	×	×	×	×	
lovsk	SV	56.73	61.07	48.5	140.7	−13.31					×	×	×	×	×	×
lovsk	VD	56.73	61.07	48.5	140.7	−13.31	×	×	×	×						
ria	VI	48.52	236.58	54.2	293.0	16.09	×	×	×	×	×	×	×		×	×
vostok	VK	43.68	132.17	32.8	198.1	4.92	×	×	×	×	×	×	×	×	×	×
veen	WI	52.82	6.67	54.2	91.2	−19.26	×	×	×	×	×	×				
-Kobenzl	WIE	48.27	16.32	47.9	98.2	−17.25	×	×	×	×	×	×	×	×	×	×
st	WN	53.75	9.07	54.6	94.1	−19.65	×	×	×	×	×	×	×	×	×	×
sk	YA	62.02	129.72	51.0	193.8	5.83	×	×							×	
ent	TK	41.33	69.62	32.3	144.0	−8.97					×	×	×	×	×	×
ent	YB	41.33	69.62	32.3	144.0	−8.97	×	×	×	×						
no-Sakhalinsk	YUZ	46.95	142.72	36.9	206.7	7.53	×	×	×	×	×	×			×	×

Previous workers (for example, Anderssen *et al.* 1970) have taken the field value at the hour immediately before the s.s.c. to represent the baseline value. This places undue emphasis on one value and serious errors can result. For example, the daily variation itself changes from day to day. Accordingly, there is no guarantee that the contribution due to the daily variation at this data point has been exactly removed. Clearly erroneous baseline values may cause appreciable errors in the estimates throughout the storm. Furthermore, statistical testing for the significant parameters of the model is undermined.

For the storms considered here, the baseline value was taken to be the arithmetic mean of the field for several quiet days immediately preceding the storm. For the March 1970 storm, because of the lack of data and the nature of the disturbance, it was necessary to use data from the quiet days after the storm, when the field values had decayed back to their undisturbed level. It was found that this approach, though by no means perfect, gave a significant improvement on the single value estimate.

Finally, a simple check on the reliability of the calculated baseline was performed. This is

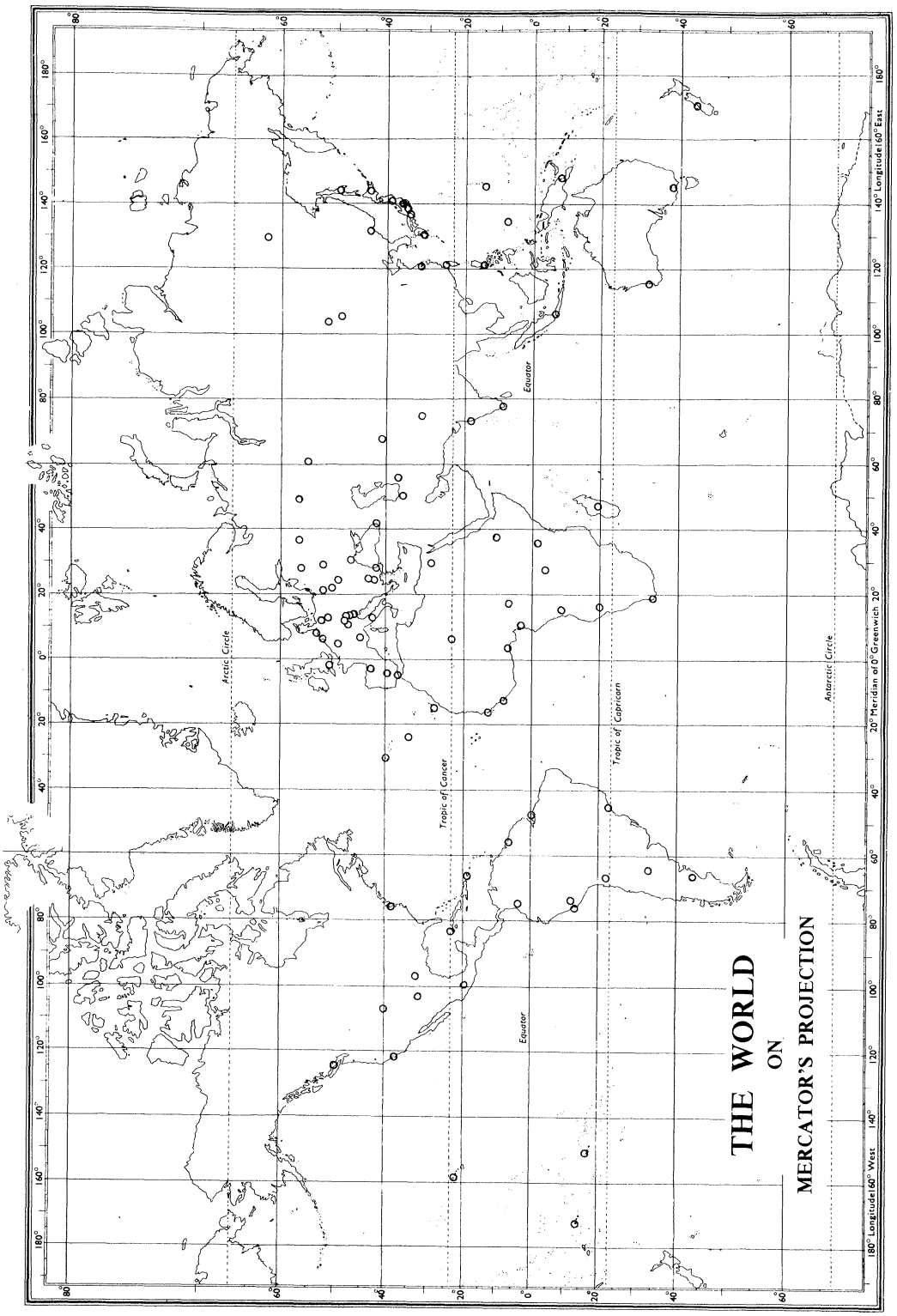

FIGURE 1. Distribution of observatories used in Dst analysis. The map is based on an outline by courtesy of George Philip & Son Ltd.

because an observatory record either may not have had S sufficiently filtered out, or the record generally may be too noisy to determine a reliable baseline value. The standard deviation of the treated data about the baseline value was calculated for the quiet period from which the baseline was previously estimated. If the standard deviation exceeded a given value, G, the record was removed from the analysis. The value of G for Z data is given by the empirical formula, $G = 20\,|\cos\theta| + 10$, and for X data, $G = 25\sin\theta + 5$. Given that the P_1 harmonic term for the Earth's main field is dominant, these formulae make some allowance for the variation of the field values with latitude. So, although G is somewhat arbitrary, it is designed to remove only records that have very unreliable calculated baseline values. In fact, it was found that this empirical test removed only a very small proportion of records, but it was nevertheless regarded as important. The precise details of S and baseline estimation for each storm are discussed in §5 below.

Detailed plots of all observatory records were made. These consisted of the smoothed data curve superimposed on the raw data curve, together with the baseline to provide a visual check. Estimates of the power spectrum of smoothed and untreated data were also plotted together. Thus some indication of the success, or otherwise, of the data treatment for each site was readily obtained. Examples of these plots are shown for each storm. The examples chosen reflect the general observatory distribution over the Earth, and illustrate the varying nature of S as, for example, from coastal to inland sites.

A further useful test on the S removal is possible by studying the nature of $e_1(t) + i_1(t)$ (for X data), or $e_1(t) - 2i_1(t)$ (for Z data), for the simple P_1 harmonic model. If S is not effectively removed it is likely that a daily variation will exist in the middle and tail sections of the recovery phase.

4. Method of analysis

Lahiri & Price (1939) showed that the geomagnetic field corresponding to the scalar potential Ω may be expressed in component form. Specifically, at the surface of the Earth,

$$\left.\begin{aligned} X_{r=a} &= -B_\theta(a) = \sum_{n=1}^{\infty}\sum_{m=-n}^{+n}\{e_n^m(t) + i_n^m(t)\}\frac{\partial}{\partial\theta}\{P_n^m(\cos\theta)\}\,\mathrm{e}^{\mathrm{i}m\phi},\\ Y_{r=a} &= B_\phi(a) = \sum_{n=1}^{\infty}\sum_{m=-n}^{+n}\{e_n^m(t) + i_n^m(t)\}\,P_n^m(\cos\theta)\,\frac{\partial}{\partial\phi}(\mathrm{e}^{\mathrm{i}m\phi}),\\ Z_{r=a} &= -B_r(a) = \sum_{n=1}^{\infty}\sum_{m=-n}^{+n}\{ne_n^m(t) - (n+1)\,i_n^m(t)\}\,P_n^m(\cos\theta)\,\mathrm{e}^{\mathrm{i}m\phi}. \end{aligned}\right\} \tag{4.1}$$

From the set of equations (4.1), it can be seen that a knowledge of the magnetic field components X and Z, from one site, is sufficient to produce estimates of the first harmonic of the external and internal parts of the field. For each extra site-data sequence available it is possible theoretically to include a further harmonic in the analysis.

Physical arguments and results from earlier work on modelling Dst variations to a Legendre polynomial series indicate that odd harmonics of low degree, particularly the P_1 term, are predominant. Nevertheless, it is useful to ascertain how important the higher degree harmonics are. This information enables a model that uses the least number of statistically significant harmonics to be produced.

The method adopted here to produce estimates of the coefficients in the Legendre expansion, together with confidence limits, follows that detailed by Mood & Graybill (1963), and Anderssen & Seneta (1969). The set of equations (4.1), when used to estimate the harmonic components of the external and internal parts of the variation field, are in practice truncated to a predetermined value M. The highest degree harmonic can then be discarded to produce a second model containing $M-1$ parameters. If the model with fewer parameters is found to represent the data as well as the M parameter model, in a statistical sense, then it is adopted. The process of removing the highest degree harmonic and testing the resulting model against the previous one is continued until the model containing the least number of statistically significant parameters is found.

Imposing a finite limit M on the series in equations (4.1) we have

$$\left.\begin{aligned} X &= \sum_{m=1}^{M} \{e_{2m-1}+i_{2m-1}\}\frac{\mathrm{d}}{\mathrm{d}\theta}P_{2m-1}(\cos\theta), \\ Z &= \sum_{m=1}^{M} \{(2m-1)\,e_{2m-1}-2mi_{2m-1}\}\,P_{2m-1}(\cos\theta). \end{aligned}\right\} \tag{4.2}$$

In terms of data from a group of observatories, equations (4.2) may be rewritten as

$$d_j(t) = \sum_{m=1}^{M} x_{jm}\beta_m(t) + S_j(t) + B_j + \gamma_j(t), \tag{4.3}$$

where d_j is the observatory data. In these equations j denotes the index of a given observatory, M is the total number of harmonics to be used in the model ($M \leqslant J$, where J is the total number of sites supplying data at a given time t), x_{jm} represents the Legendre harmonic (for X data analysis) or the θ derivative of the Legendre polynomial (for Z data analysis) of degree $2m-1$ for the jth site; β_m represents either $(e_{2m-1}+i_{2m-1})$ or $(2m-1)\,e_{2m-1}-2mi_{2m-1}$ depending upon whether the data, d, is the X or Z field component. S_j is the periodic component due to the daily variation at the jth site. B_j is the baseline value, i.e. that constant part of the field at the jth site not due to Dst. Finally, γ_j is a measure of the error.

In real Dst data the daily variation is not constant throughout the storm, but is modulated by aperiodic variations. The manner in which these aperiodic variations modulate the daily variation is poorly understood, and this disturbed daily variation, S_{D}, is particularly difficult to estimate reliably. The solution adopted by some previous workers was to remove the S_{q} variation as an approximation to S_{D}. In practice this approach seems to be realistic and a similar method is adopted here, where an estimate of the quiet day daily variation is used. Undoubtedly some variation due to S_{D} remains, but the error incurred is considered to be acceptably small.

For the storms considered here, data is analysed at hourly intervals. Each hourly value being the mean hourly value, centred at the half hour point. Thus the explicit time dependence in (4.3) is now omitted, since subsequent work only concerns the analysis of data at a given time step. Equation (4.3) thus reduces to

$$y_j = \sum_{m=1}^{M} x_{jm}\beta_m + \gamma_j, \tag{4.4}$$

where y_j is the treated observatory data ($y_j = d_j - S_j - B_j$), or more simply in matrix notation

$$Y = X\beta + \gamma, \tag{4.5}$$

where X is of full rank M.

It can be shown that if the γ_j are independently and identically distributed normal variables,

with zero mean, and variance σ^2 then the maximum likelihood estimates $\hat{\beta}$, $\hat{\sigma}^2$ of β and σ^2 are given by

$$\hat{\beta} = (X^{\mathrm{T}}X)^{-1}X^{\mathrm{T}}Y, \tag{4.6}$$

$$J\sigma^2 = (Y - X\hat{\beta})^{\mathrm{T}}(Y - X\hat{\beta}). \tag{4.7}$$

It may be noted that $\hat{\beta}$ is also the least squares estimate of β. Further manipulation of (4.7) yields

$$J\sigma^2 = Y^{\mathrm{T}}(I - X(X^{\mathrm{T}}X)^{-1}X^{\mathrm{T}})\,Y. \tag{4.8}$$

It can be shown that $\hat{\beta}$ is distributed as the M-variate normal distribution with mean β and covariance matrix $(X^{\mathrm{T}}X)^{-1}\sigma^2$, and that $\hat{\beta}$ is independent of $(J-M)\,\hat{\sigma}^2/\sigma^2$, which is distributed as chi square with $J-M$ degrees of freedom. This allows the derivation of a $(1-\alpha)\times 100\,\%$ confidence interval for β_m, given by

$$\beta_m = \hat{\beta}_m \pm t_{J-M}(\alpha)\,\{J\hat{\sigma}^2(J-M)^{-1}\,(X^{\mathrm{T}}X)^{-1}_{m,m}\}^{\frac{1}{2}}, \tag{4.9}$$

where $t_{J-M}(\alpha)$ is the two-tail α point of the t distribution (table IV, Mood & Graybill 1963), with $J-M$ degrees of freedom, and $(X^{\mathrm{T}}X)^{-1}_{m,m}$ is the m,mth element of the matrix $(X^{\mathrm{T}}X)^{-1}$. The standard error of β_m is given by

$$\text{s.e.}\,(\beta_m) = \{J\hat{\sigma}^2(J-M)^{-1}(X^{\mathrm{T}}X)^{-1}_{m,m}\}^{\frac{1}{2}}. \tag{4.10}$$

So by using equations (4.6) and either (4.9), or (4.10), β may be estimated within given confidence limits.

So far, the mathematical formulation has been based on the implicit assumption that Dst variations are correctly described by these M parameters. It is possible to test this hypothesis by comparing the M parameter model to a model containing N parameters $(0 < N < M)$; that is, given the general model of equation (4.5) test the hypothesis that $\beta_{\mathrm{b}} = 0$, without restricting β_{a}, where

$$Y = X\beta + \gamma = (X_{\mathrm{a}}, X_{\mathrm{b}})\begin{pmatrix}\beta_{\mathrm{a}}\\ \beta_{\mathrm{b}}\end{pmatrix} + \gamma, \tag{4.11}$$

with

$$\beta_{\mathrm{a}} = \begin{pmatrix}\beta_1\\ \vdots\\ \beta_N\end{pmatrix}, \quad \beta_{\mathrm{b}} = \begin{pmatrix}\beta_{N+1}\\ \vdots\\ \beta_M\end{pmatrix}, \quad \beta = \begin{pmatrix}\beta_{\mathrm{a}}\\ \beta_{\mathrm{b}}\end{pmatrix}, \quad X = (X_{\mathrm{a}}, X_{\mathrm{b}}).$$

It should be noted that the $\beta_{N+1}, \beta_{N+2}, \ldots, \beta_M$ coefficients do not necessarily correspond to the higher degree Legendre polynomials in the model. Clearly X and β may be arranged such that the required parameters constitute the matrix β_{b}.

A test statistic for the hypothesis that $\beta_{\mathrm{b}} = 0$ is

$$F^{(M,N)} = (\hat{\sigma}^2_{\mathrm{a}}/\sigma^2 - 1)\,(J-M)/(M-N), \tag{4.12}$$

where $\hat{\sigma}^2_{\mathrm{a}}$ and $\hat{\sigma}^2$ are respectively the maximum likelihood estimators of σ^2 for an N and an M parameter model, and may be calculated from (4.8).

Now if $F^{(M,M)} > F_{M-N,J-M}(\alpha)$, the new model containing N parameters may be abandoned in favour of the old M parameter model. Note that $F_{M-N,J-M}(\alpha)$ is the upper 100α percentage point of the F distribution with degrees of freedom $M-N$, $J-M$ (table V, Mood & Graybill 1963). However, if $F^{(M,N)} < F_{M-N,J-M}(\alpha)$, the new N parameter model may be accepted and this in turn tested against further models containing less parameters. This process leads eventually to the model containing the minimum number of parameters that are statistically significant in Dst variations.

PHILOSOPHICAL TRANSACTIONS OF THE ROYAL SOCIETY A MATHEMATICAL, PHYSICAL & ENGINEERING SCIENCES

5. The storm analyses

A total of six storms have been analysed. Table 1 lists the observatories used in each analysis, and also shows the geographic and geomagnetic coordinates of these sites, together with the associated values of ψ. Figure 1 shows the positions of these sites on a world map. Unfortunately, these observatories are poorly distributed, being mainly concentrated in the northern hemisphere, with very few sites in the oceans or southern hemisphere. It should be noted that broken observatory sequences may be used, provided that realistic estimates of the baseline value and S for that site can be found.

In middle and low latitudes, Dst variations are generally accepted to be due to a ring current, and the field produced is non-localized and of a uniform nature. In high latitudes, however, the variation field is localized and irregular due to the intense electric currents flowing in the ionosphere around the auroral zones. Furthermore, the daily variation in the high latitude region is significantly disturbed. To study the global large scale field variations only observatory data from sites within $\pm 55°$ of the geomagnetic equator were used.

To some extent the $\pm 55°$ latitude limit is arbitrary. Initially, site data from within $\pm 60°$ of the geomagnetic equator were used, but it was found that because of contamination from auroral effects significantly better results are found from sites within $\pm 55°$ latitude of the geomagnetic equator. In fact, there is a trade-off such that the $55°$ limit probably approaches the widest limit available to analyse the data effectively. This is because increasing the latitude limit allows more sites to be included, which in turn should lead to more reliable estimates of β. However, the data from these high latitude sites is difficult to analyse because of the auroral effects and S_D smoothing difficulties, so that its inclusion leads to less reliable estimates of β, and the statistical testing for significant parameters is weakened.

In all cases an initial model containing P_1, P_3, P_5 and P_7 Legendre polynomials was used for both X and Z data. This model was tested against a P_1, P_3, P_5 representation, which in turn was tested against a P_1, P_3 model and so on. The results of the tests were analysed to determine which model contained the least number of statistically significant parameters. It should be noted that, initially, Legendre polynomials of low even degree (2, 4, 6) were also used but found to be unimportant in the representation of Dst data. In the final analysis only low odd degree harmonics were used.

In determining the appropriate model for X and Z data, only the recovery phase of each storm was used to calculate the F statistic. This is because during the initial phase of a storm, high frequency variations are dominant, and the field values are much affected by the near-surface lateral variations in the Earth's conductivity structure. During the recovery phase, longer period variations are important, and the associated induced currents penetrate deeper into the Earth where the assumption of spherical symmetry has greater validity.

Estimates of β and its associated error at a given time step can now be produced. For the first harmonic $\hat{\beta}_1(X) = \hat{e}_1 + \hat{i}_1$ and $\hat{\beta}_1(Z) = \hat{e}_1 - 2\hat{i}_1$. Simple manipulation produces expressions for $\hat{e}_1$ and $\hat{i}_1$, and to obtain estimates of the standard errors of $\hat{e}_1$ and $\hat{i}_1$, we assume that X and Z Dst field values are independently distributed. Therefore, $\hat{\beta}(X)$ and $\hat{\beta}(Z)$ are independently distributed and the standard errors of $\hat{e}_1$ and $\hat{i}_1$ are given by

$$\left.\begin{aligned} \text{s.e.}\,(\hat{e}_1) &= [(\tfrac{2}{3})^2\{\text{s.e.}\,\hat{\beta}_1(X)\}^2 + (\tfrac{1}{3})^2\{\text{s.e.}\,\hat{\beta}_1(Z)\}^2]^{\frac{1}{2}} \\ \text{s.e.}\,(\hat{i}_1) &= [(\tfrac{1}{3})^2\{\text{s.e.}\,\hat{\beta}_1(X)\}^2 + (\tfrac{1}{3})^2\{\text{s.e.}\,\hat{\beta}_1(Z)\}^2]^{\frac{1}{2}}. \end{aligned}\right\} \tag{4.13}$$

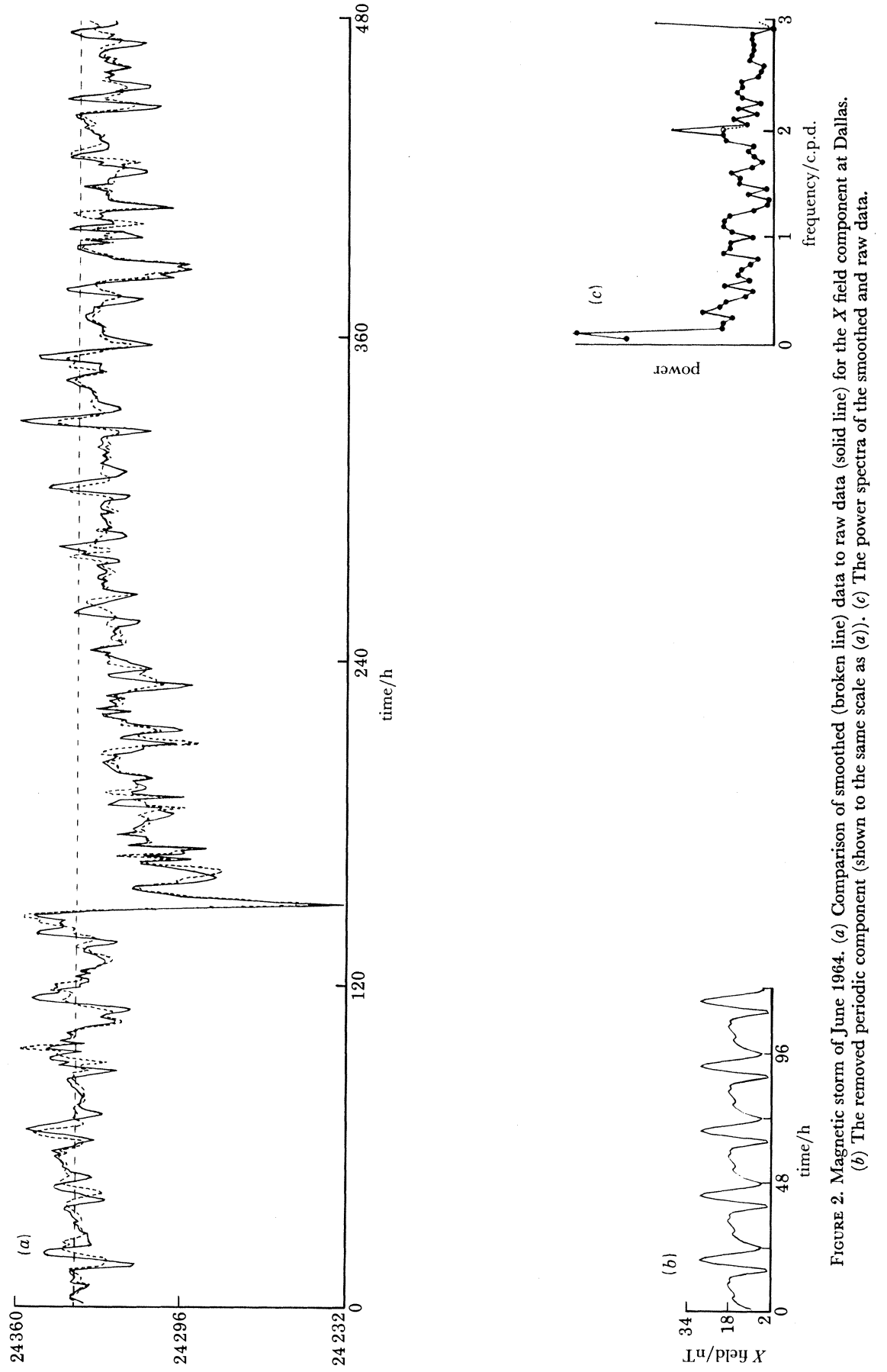

FIGURE 2. Magnetic storm of June 1964. (*a*) Comparison of smoothed (broken line) data to raw data (solid line) for the *X* field component at Dallas. (*b*) The removed periodic component (shown to the same scale as (*a*)). (*c*) The power spectra of the smoothed and raw data.

PHILOSOPHICAL TRANSACTIONS OF THE ROYAL SOCIETY A MATHEMATICAL, PHYSICAL & ENGINEERING SCIENCES

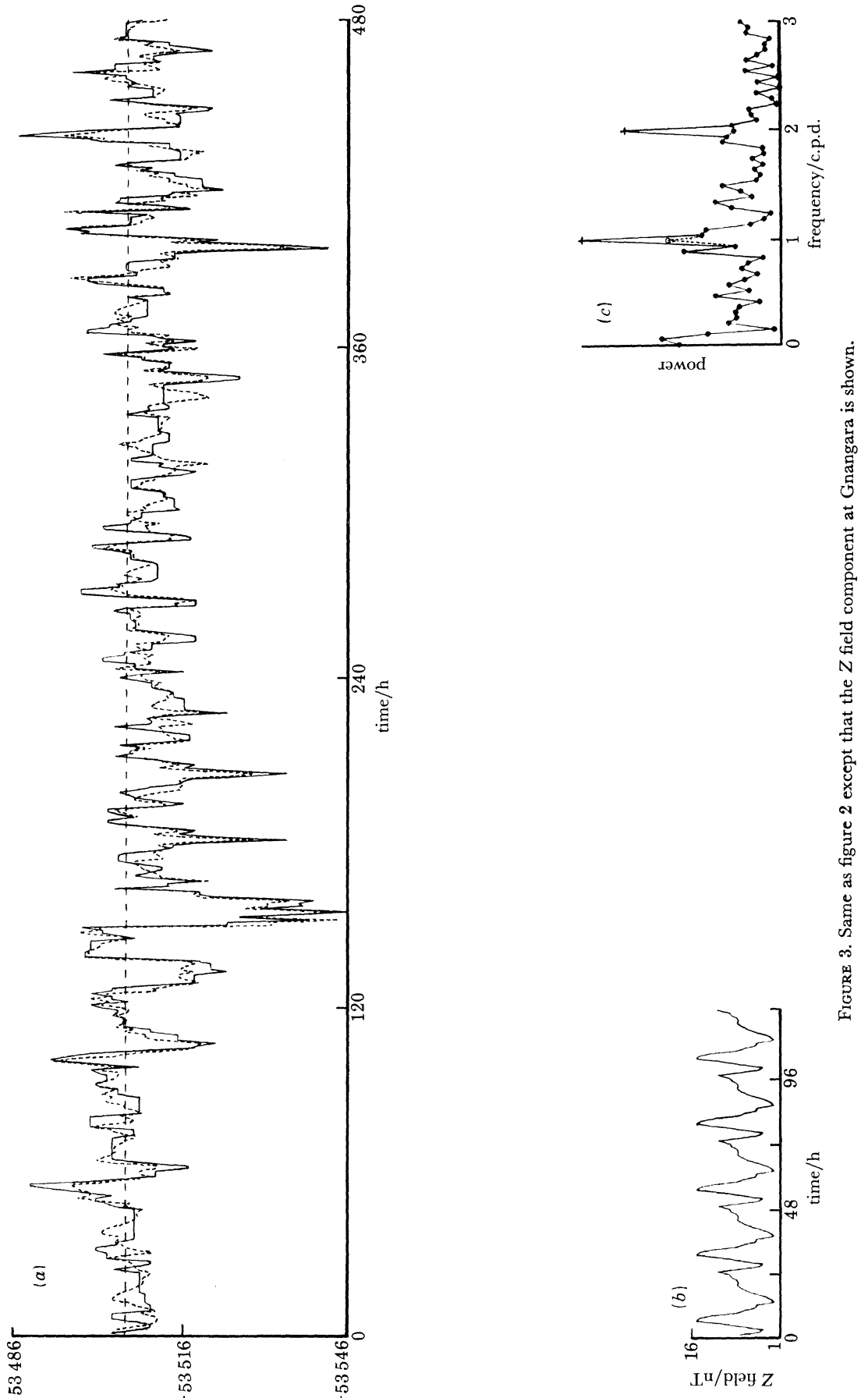

FIGURE 3. Same as figure 2 except that the Z field component at Gnangara is shown.

PHILOSOPHICAL TRANSACTIONS OF THE ROYAL SOCIETY A MATHEMATICAL, PHYSICAL & ENGINEERING SCIENCES

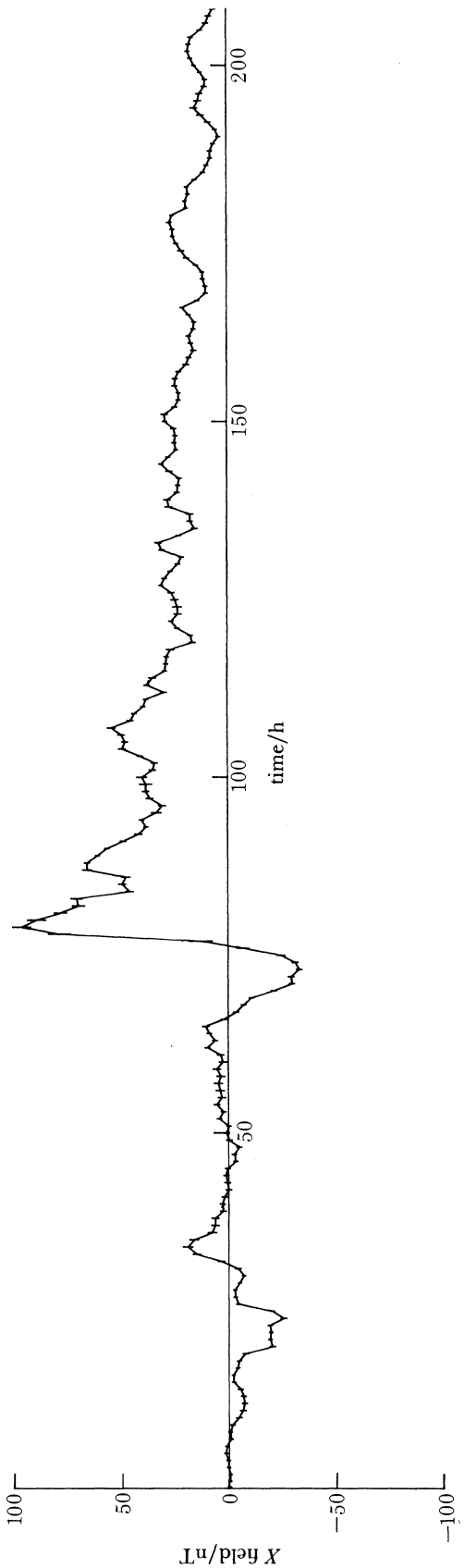

FIGURE 4. P_1 harmonic of the 3 parameter model of the X data for the period beginning 7 June 1964.

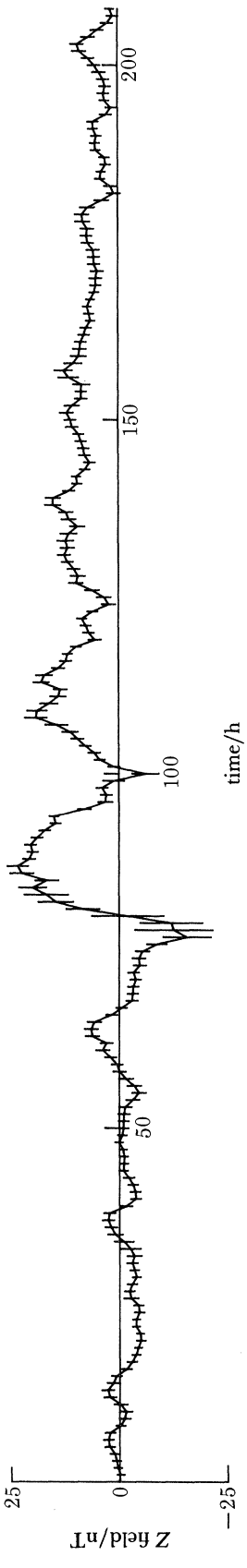

FIGURE 5. P_1 harmonic of the 2 parameter model of the Z data for the period beginning 7 June 1964.

PHILOSOPHICAL TRANSACTIONS OF THE ROYAL SOCIETY A MATHEMATICAL, PHYSICAL & ENGINEERING SCIENCES

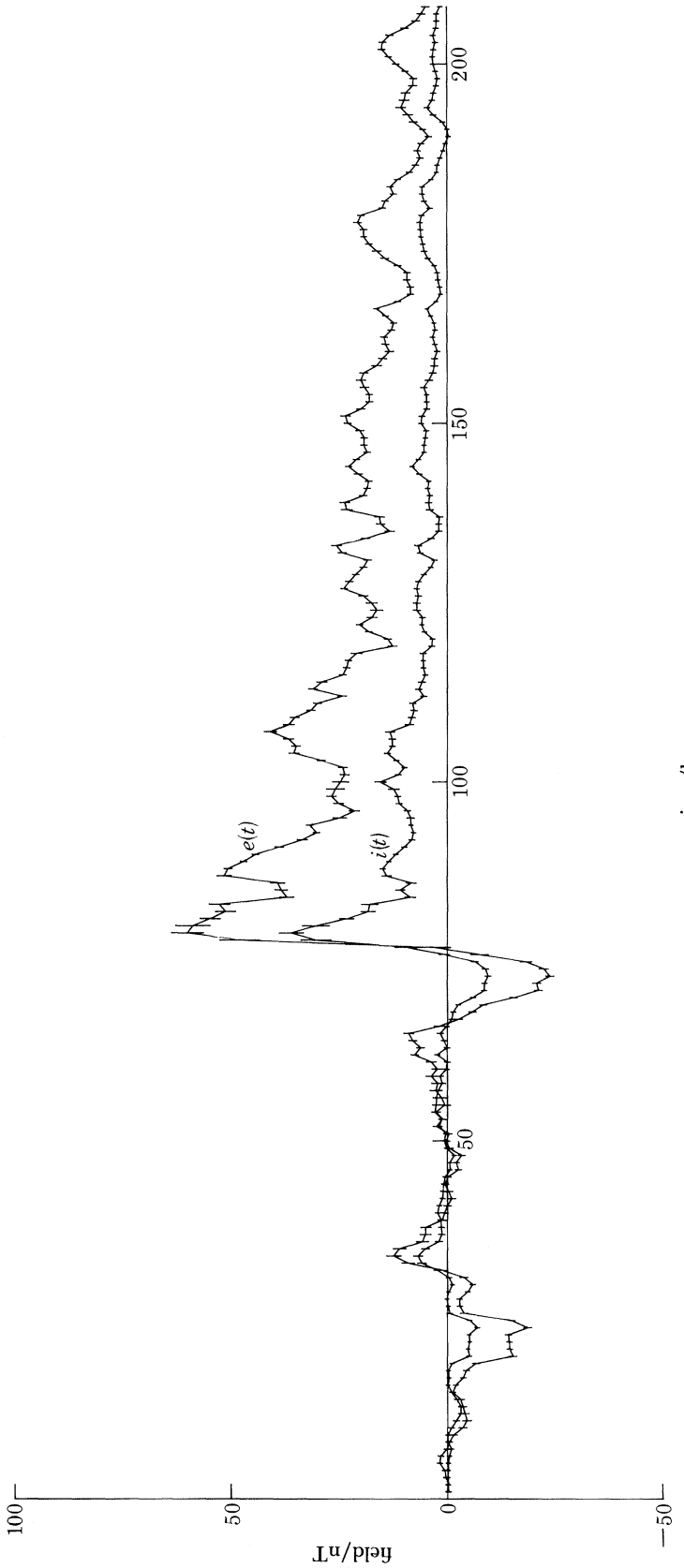

FIGURE 6. The P_1 component of the external and internal parts of the Dst field for the period beginning 7 June 1964.

PHILOSOPHICAL TRANSACTIONS OF THE ROYAL SOCIETY A MATHEMATICAL, PHYSICAL & ENGINEERING SCIENCES

5.1. *The storm of* 7 *June* 1964

Table 1*a* in I.A.G.A. Bulletin no. 12 s2 lists a sudden storm commencement at 18 h 52 min 7 June. Table 1*b* of the same bulletin lists 'not checked' sudden storm commencements on 9 June and 10 June. However, Sugiura & Poros (1971) have produced graphs of the hourly values of equatorial Dst. These indicate a well defined, though small, storm beginning late on 9 June. Accordingly, hourly values of the magnetic field components were gathered for the period 4 June–23 June inclusive. It is clear from the data that a major disturbance occurs during this period. The storm does not have a clear entry, and its amplitude is rather smaller than those of previously analysed storms.

S was calculated with data from days 4, 5, 6, 13, 14, 15, 16, 17, 18, 19, 22 and 23 June. Days 20 and 21 were not included because of a slight disturbance during that period. Only days containing unbroken data were used and, for a given site, at least 7 of these days were required to estimate S. The baseline value taken for each data sequence was the arithmetic mean field value for the first 3 days (72 h) of that record. The site sequence was discarded from the analysis if more than 18 of these values were missing.

Figure 2 shows an example of the X field component for the 20-day period. The site shown is Dallas. An example of the Z component, showing data from Gnangara, is given in figure 3. Both sites illustrate the typical noisy nature of this storm. The inclusion of estimated baselines (dashed lines) on the diagrams helps to identify the storm and its general form. The daily variation is relatively weak in both records, though its existence is shown in the power spectrum of the untreated data. The success of the least squares finite Fourier series technique for the removal of S is shown by comparing the power spectra of the treated and untreated data.

After the baseline had been determined, and S removed from each site data sequence, there were 65 records of X data and 58 records of Z data available for analysis. Details of the actual F statistics for the recovery phase of the storm, from 161 to 280 h inclusive, are given by Marshall (1980). For the overall recovery phase the X data is represented by the least number of statistically significant parameters by the P_1, P_3, P_5 model, whereas the Z data are best represented by the P_1, P_3 model only.

The P_1 harmonic is found to be dominant, both for the X and Z analyses. Figures 4 and 5 show respectively the P_1 harmonic of the X (3 parameter model) and Z (2 parameter model) data. The X component is much better defined. In terms of magnitude, the error bounds for the first harmonic during the recovery phase are of order 1 or 2 nT for both X and Z components, whereas the field variation on the X graph is about 150 nT, but only 60 nT for the Z graph.

The major field variations for this storm occur between 150 and 160 h in the data sequence. After this point the recovery phase begins, with both X and Z variations showing a rather irregular recovery, this is in accordance with the typical site records for this storm shown in figures 2 and 3.

Values of $e_1(t)$ and $i_1(t)$, together with their associated standard errors, are displayed in figure 6. Throughout the storm the morphology of the induced field is similar to the external, forcing field. At the beginning of the disturbance, $i_1(t)$ responds very quickly to changes in $e_1(t)$. Later in the storm the internal field is rather more sluggish and gives the impression of being a smoothed, reduced version of the external field. It is encouraging to note that there appears to be no appreciable daily variation in the middle and later parts of the recovery phase. Similar diagrams of $e_1(t)$ and $i_1(t)$, not shown here, of the single parameter P_1 model, also fail to reveal any prevalent 24 h variation.

This particular storm is small in amplitude compared with previously analysed disturbances, though the recovery phase is clearly observable for approximately 5 days after the storm onset before the field values approach the pre-storm undisturbed state. This is important because it shows that even small amplitude storms contain measurable variations at frequencies down to approximately 0.2 cycle/day (c.p.d.). These variation fields penetrate deep into the upper mantle and are of importance to upper mantle conductivity studies.

5.2. *The storm of* 17 *April* 1965

The data sequence for the period 13 April–2 May consists of approximately 4 quiet days before the onset of the storm. The entry was reasonably clear and was followed by a major variation in the field during 5–12 h on 18 April. This was followed by a relatively smooth recovery phase lasting for about 200 h. In this case S was calculated with data from 13 April–16 April, and from 23 April–2 May. The baseline was determined from the first 96 h of each record. A site was discarded unless 10 days were available to estimate S, and 72 of the 96 h were available for baselining. A total of 67 observatories finally contributed records of both X and Z components.

Figure 7 shows the X component of magnetic field measured at Hyderabad, and figure 8 displays the Z component measured at Furstenfeldbruck. In both records there exists a strong, reasonably regular, daily variation, and the unusually long recovery phase, lasting more than 15 days, can be seen.

The F statistics for the recovery phase, from 131–290 h show that the X data is represented by a P_1, P_3, P_5 model and the Z data by a P_1, P_3 model.

In common with all the storm analyses presented here, the P_1 component is dominant, and the P_3 and P_5 (in the case of X data) components are much smaller. The associated error bounds for these last two components render them virtually useless in terms of further analysis.

The P_1 component for the X and Z data are shown in figures 9 and 10 respectively. The field variation for X is 230 nT, and only 90 nT for Z, and as was found for the 1964 storm, the X component is much better defined. In fact, for the recovery phase, the absolute errors for the Z field component are generally about twice as large as those associated with the X component.

An interesting feature of the Z component is the two peaks in the recovery phase at approximately 158 and 180 h in the sequence. A typical example of the Z data for this period is shown in figure 8. The two peaks, after S has been removed, can be clearly seen. The X data seems unaffected at the time of the first peak in Z, but does have a coincident peak at about 180 h.

The values of the separated fields, $e_1(t)$ and $i_1(t)$, are shown in figure 11 for the period 16–24 April. At its maximum the external field, $e_1(t)$, reaches 119 nT, while the maximum internal field, $i_1(t)$, is only 58 nT. Compared with the 1964 storm, the recovery phase is relatively smooth, with both the external and internal fields being well defined for up to 7 days after the storm commencement. It is noticeable that at times of rapid field variation, particularly during the initial phase of the storm, the field values are not so well defined.

The peaks shown in both X and Z data for the recovery phase are also present in the separated curves. The first of these appears as a peak in the external field but as a trough in the internal field. Later on, the second disturbance appears as a peak in both the external and internal fields. Any distinct 24 h variation in the middle and later part of the recovery phase fails to show. A similar check on the results of the one parameter, P_1, model yields the same result, and it can be concluded that S has been effectively removed. The calculated baseline also appears to be quite realistic with the recovery values slowly approaching the pre-storm, undisturbed, level.

PHILOSOPHICAL TRANSACTIONS OF THE ROYAL SOCIETY A MATHEMATICAL, PHYSICAL & ENGINEERING SCIENCES

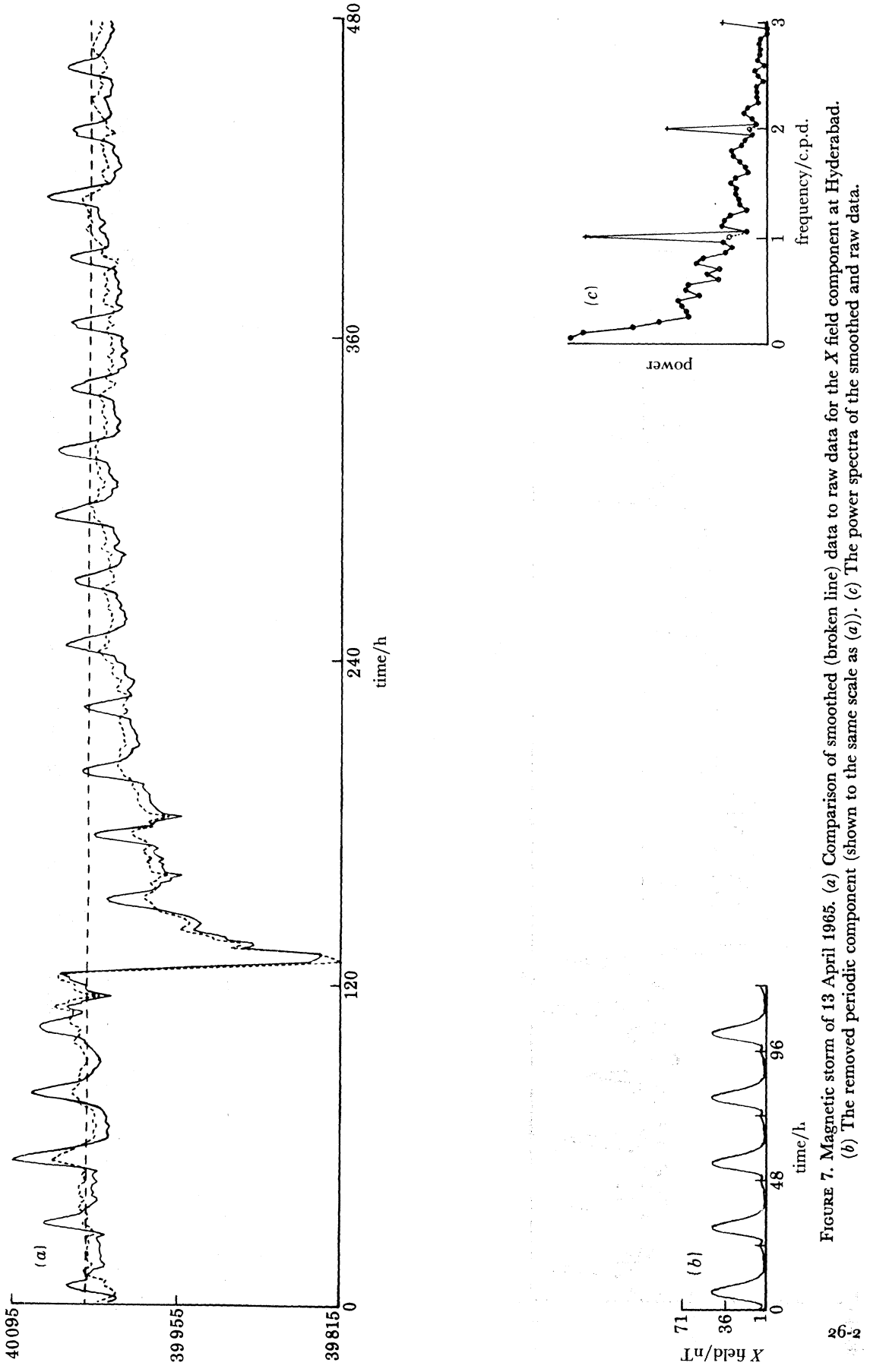

FIGURE 7. Magnetic storm of 13 April 1965. (*a*) Comparison of smoothed (broken line) data to raw data for the *X* field component at Hyderabad. (*b*) The removed periodic component (shown to the same scale as (*a*)). (*c*) The power spectra of the smoothed and raw data.

PHILOSOPHICAL TRANSACTIONS OF THE ROYAL SOCIETY A MATHEMATICAL, PHYSICAL & ENGINEERING SCIENCES

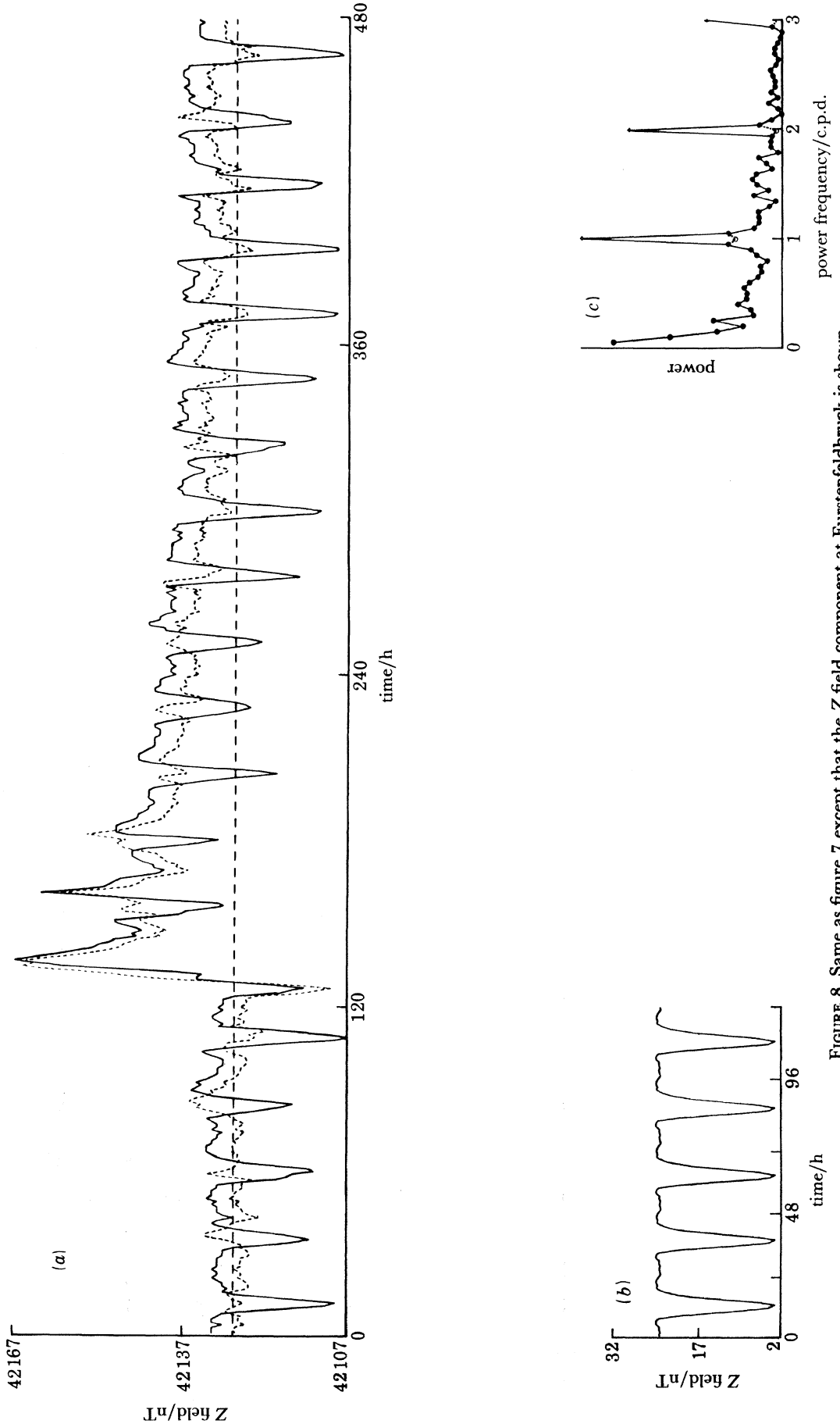

FIGURE 8. Same as figure 7 except that the Z field component at Furstenfeldbruck is shown.

PHILOSOPHICAL TRANSACTIONS OF THE ROYAL SOCIETY A MATHEMATICAL, PHYSICAL & ENGINEERING SCIENCES

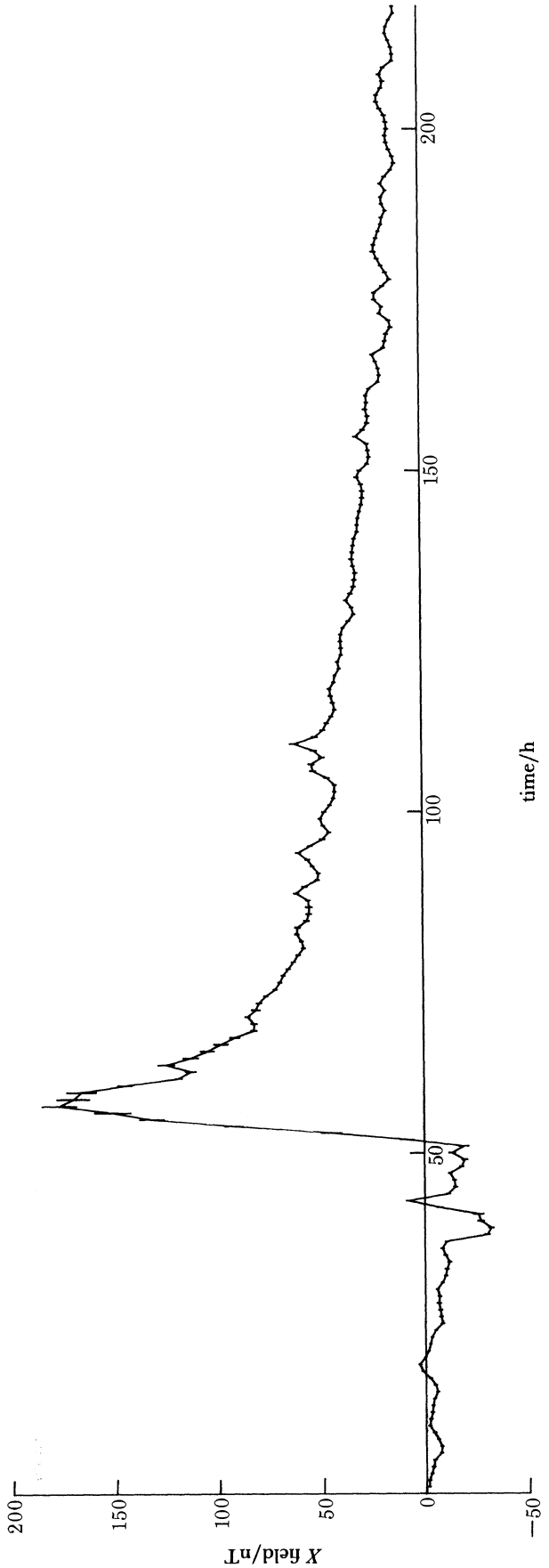

FIGURE 9. P_1 harmonic of the 3 parameter model of the X data for the period beginning 16 April 1965.

PHILOSOPHICAL TRANSACTIONS OF THE ROYAL SOCIETY A MATHEMATICAL, PHYSICAL & ENGINEERING SCIENCES

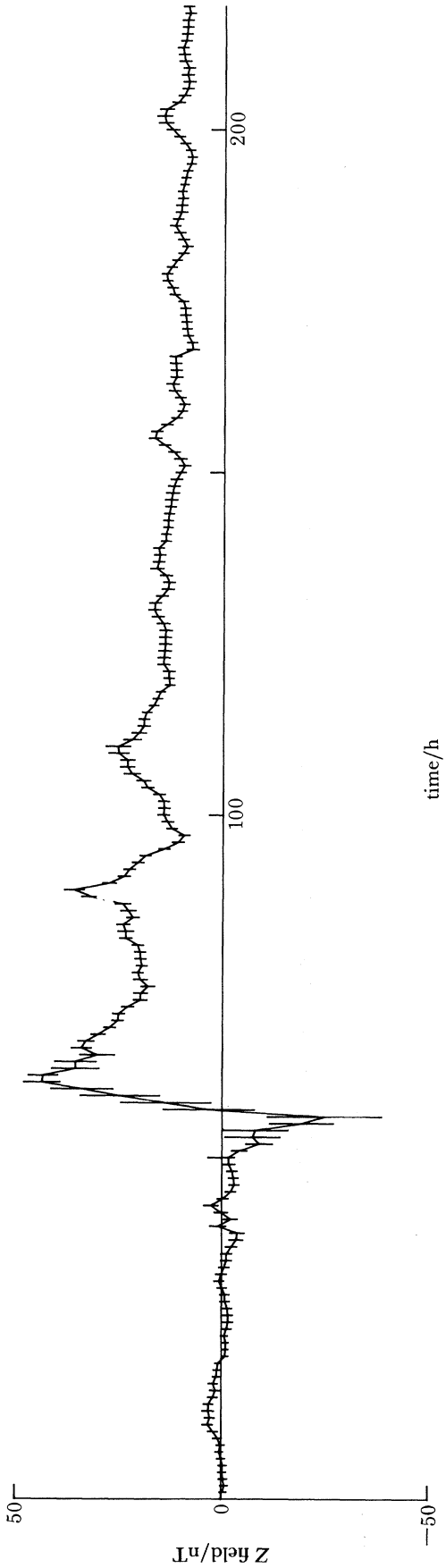

FIGURE 10. P_1 harmonic of the 2 parameter model of the Z data for the period beginning 16 April 1965.

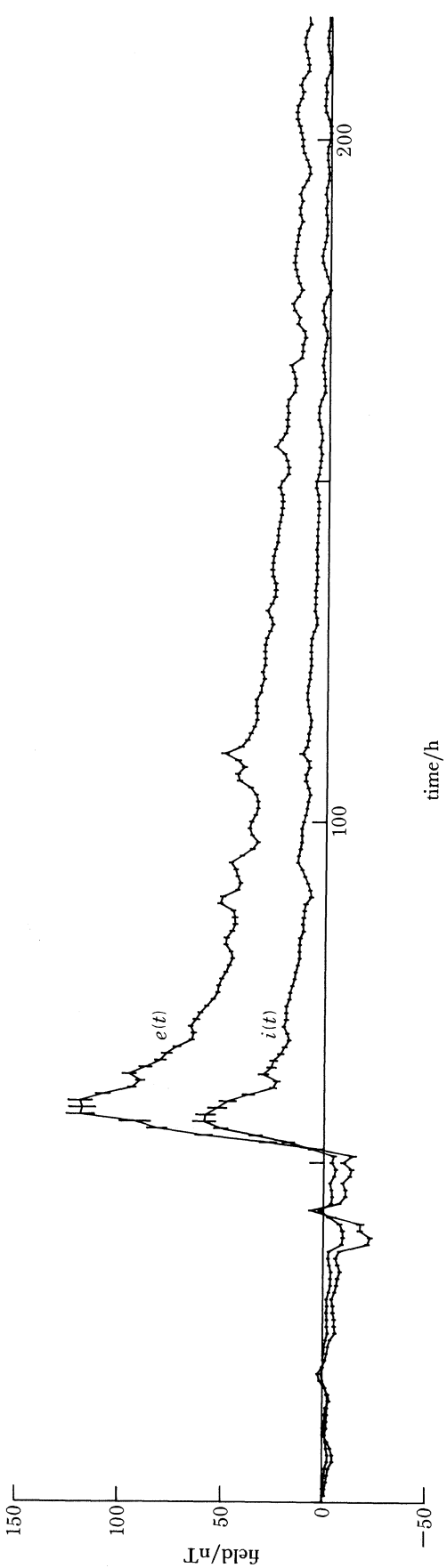

FIGURE 11. The P_1 component of the external and internal parts of the Dst field for the period beginning 16 April 1965.

PHILOSOPHICAL TRANSACTIONS OF THE ROYAL SOCIETY A MATHEMATICAL, PHYSICAL & ENGINEERING SCIENCES

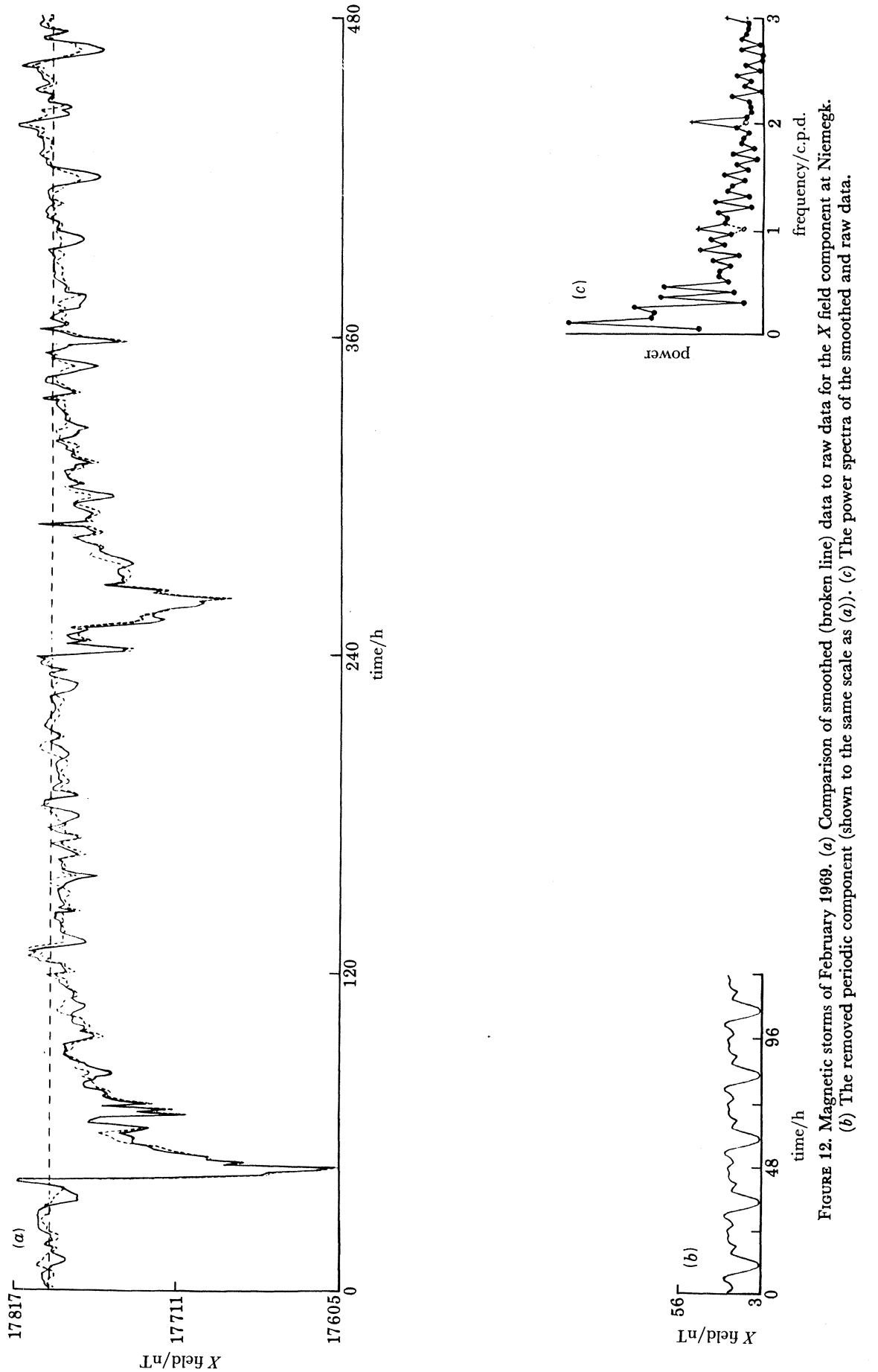

FIGURE 12. Magnetic storms of February 1969. (*a*) Comparison of smoothed (broken line) data to raw data for the *X* field component at Niemegk. (*b*) The removed periodic component (shown to the same scale as (*a*)). (*c*) The power spectra of the smoothed and raw data.

PHILOSOPHICAL TRANSACTIONS OF THE ROYAL SOCIETY A MATHEMATICAL, PHYSICAL & ENGINEERING SCIENCES

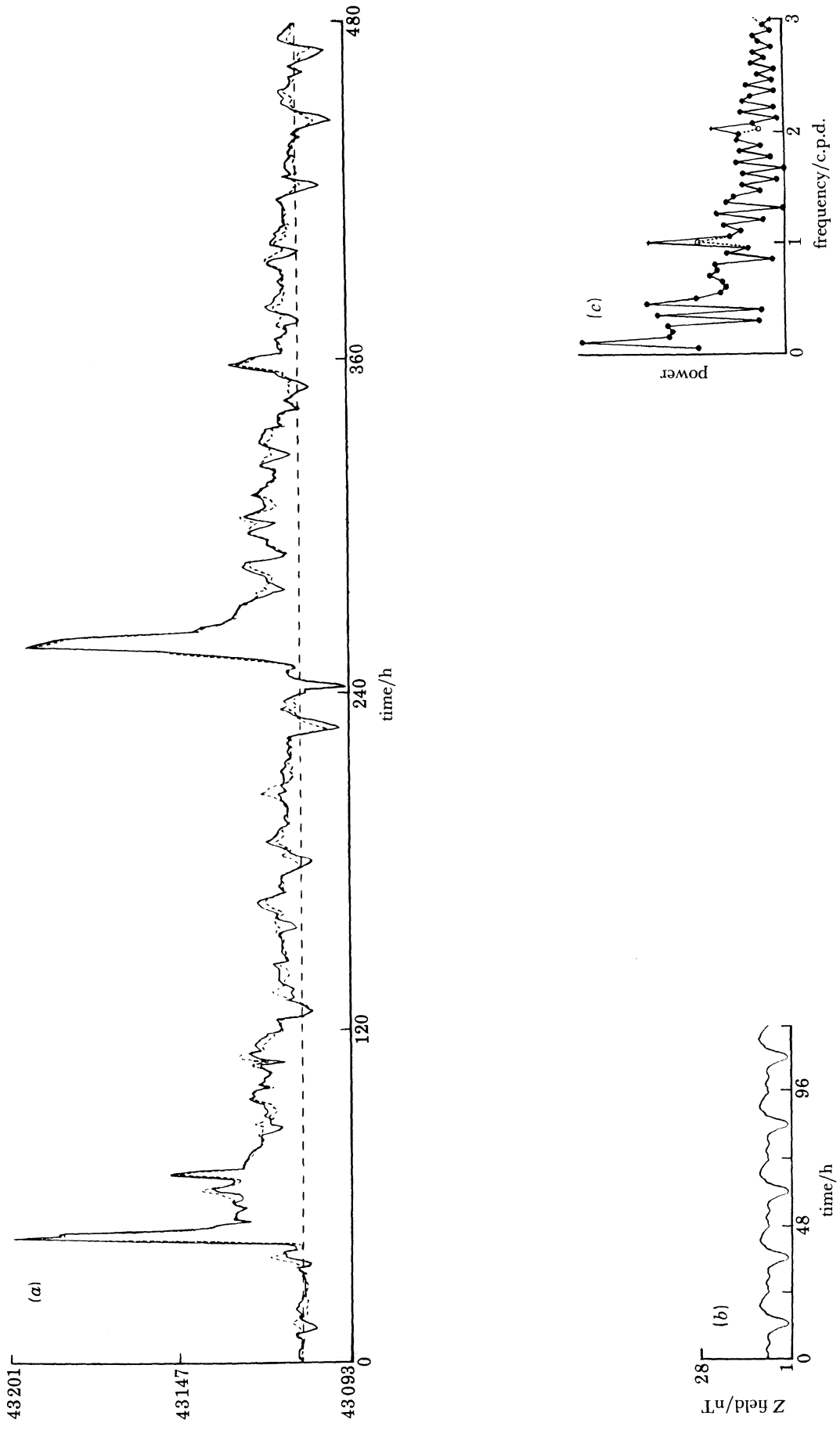

FIGURE 13. Same as figure 12 except that the Z field component at Dourbes is shown.

PHILOSOPHICAL TRANSACTIONS OF THE ROYAL SOCIETY A MATHEMATICAL, PHYSICAL & ENGINEERING SCIENCES

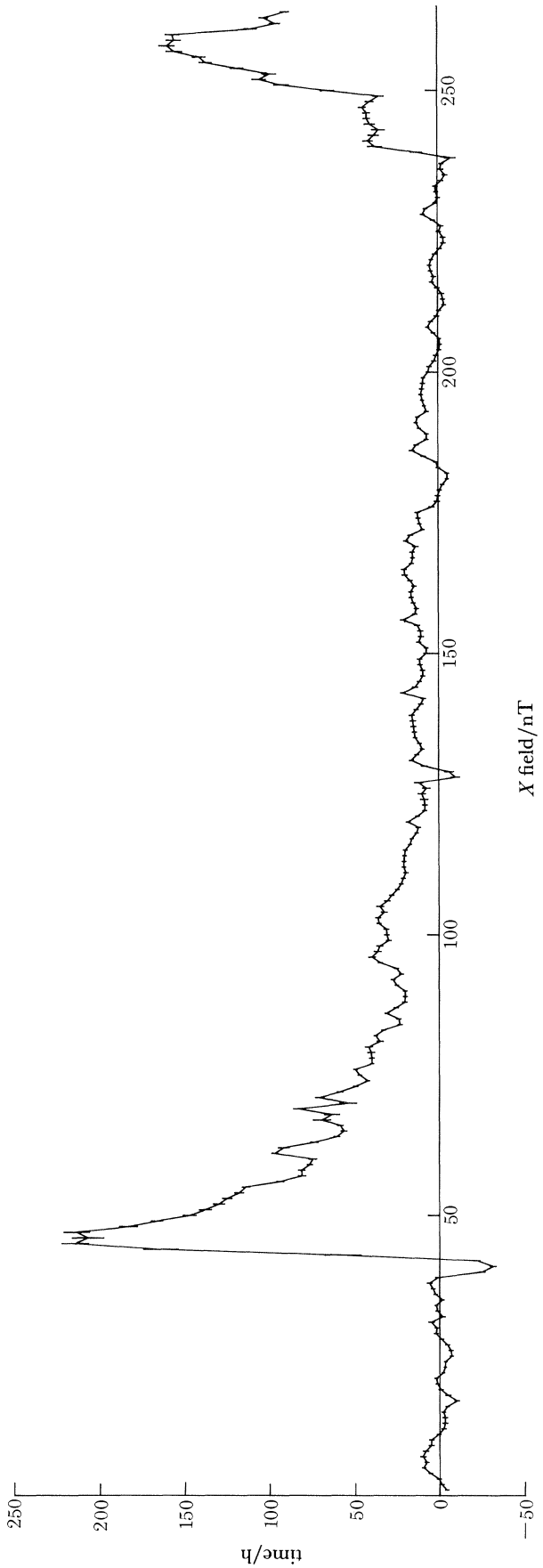

FIGURE 14. P_1 harmonic of the 3 parameter model of the X data for the period beginning 1 February 1969.

PHILOSOPHICAL TRANSACTIONS OF THE ROYAL SOCIETY A MATHEMATICAL, PHYSICAL & ENGINEERING SCIENCES

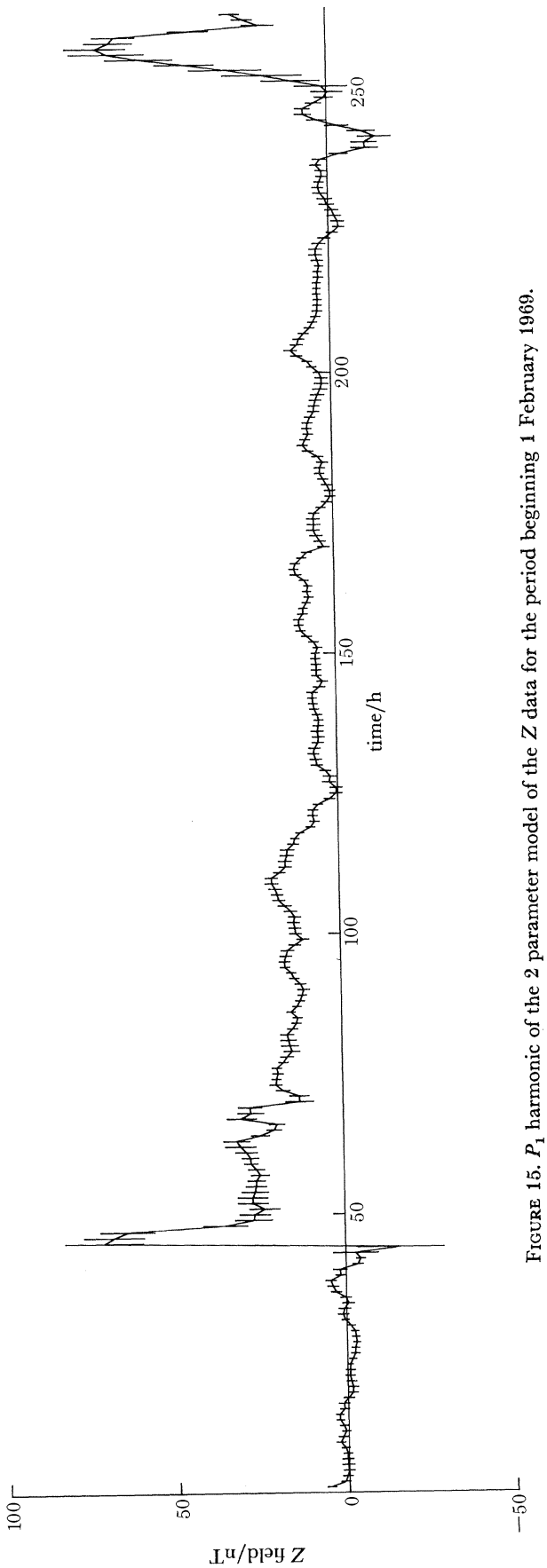

FIGURE 15. P_1 harmonic of the 2 parameter model of the Z data for the period beginning 1 February 1969.

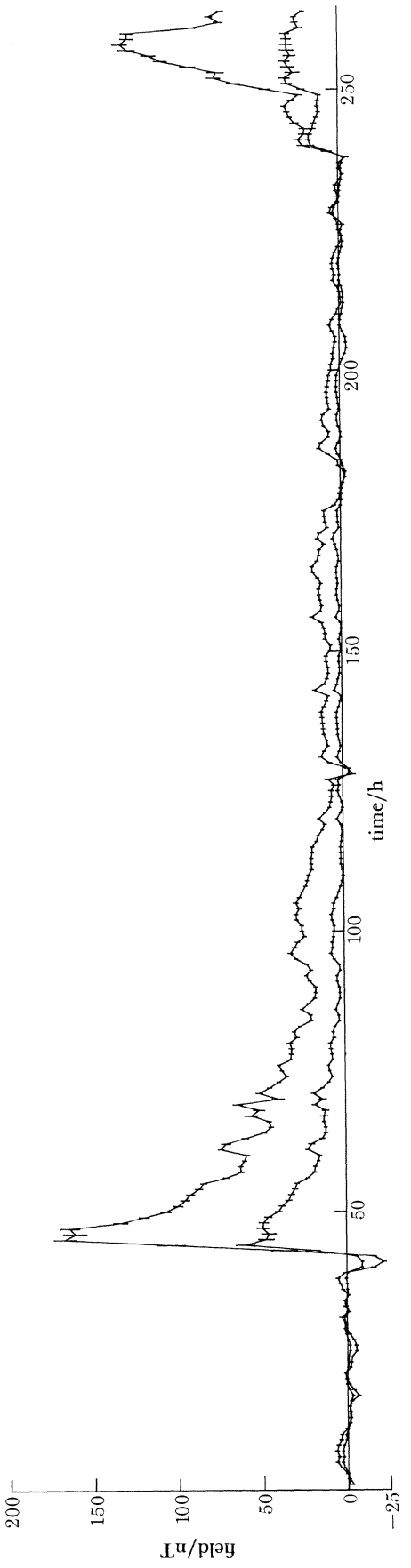

FIGURE 16. The P_1 component of the external and internal parts of the Dst field for the period beginning 1 February 1969.

5.3. *The storm of* 2 *February* 1969

For this storm, hourly values for the first 20 days of February 1969 were gathered. The storm was found to be well defined with a clear entry phase. The daily variation was calculated with data from days 1, 7, 8, 9, 16, 17, 18, 19, and 20 February, and for a given site at least 6 of these days were required to estimate S. The observatory baseline value was calculated from the first 36 h of the record, if more than 9 of these values were missing, the data sequence for that site was not used. The amount of data that was used to estimate the baseline value was smaller than for any other storm analysis presented here. Ideally, a longer undisturbed period would be used, however, only data from 1 to 20 February were available for this study. Nevertheless, the 36 h sequence used was particularly quiet (Sugiura & Poros 1971) and provided a realistic observatory baseline value. After the removal of S, and the baseline from each site data sequence, a maximum of 62 observatory records for X and 64 records for Z were available for use.

The X field component measured at Niemegk, and the Z field at Dourbes, are shown in figures 12 and 13 respectively. The clear storm entry, and steady pre-storm field values can be seen. The field approaches its undisturbed state after about 5 days from the commencement. The F statistics indicate that for the overall recovery phase, both the X and Z data are represented by the least number of statistically significant parameters with a P_1, P_3, P_5 model. However, the model taken for the Z component is the one containing only the P_1 and P_3 harmonics for reasons given below.

Figures 14 and 15 show the P_1 harmonic for X and Z from 1 to 264 h. The field variation on the X graph is 270 nT, and on the Z graph it is 120 nT. It is clear from these figures that the recovery phase, in common with all the other storms analysed here, is far better defined than the initial phase of the storm. The commencement of the following storm can be seen just before the X and Z field values have returned to the baseline value.

The separated external and internal fields are shown in figure 16. The maximum external field value is 167 nT, and the maximum internal field value is 60 nT. The general morphology of the internal field is similar to that of the external field. An inspection of figures 14–16, and of the equivalent results for the single component, P_1, model (not shown here), fails to show any distinct 24 h variation in the middle and latter parts of the recovery phase, and the removal of S appears to have been satisfactory. Furthermore, the general nature of the recovery phase, and the convergence of the field values indicates that a realistic baseline was found.

5.4. *The storm of* 10 *February* 1969

This storm was analysed from the same 20 day dataset that was compiled for the preceding storm, and removal of the daily variation and baselining done in the same manner as described there. It was found from a study of the F statistics that no model with less than 4 harmonics was entirely satisfactory in describing the X data. The F statistics for the Z field indicated that the P_1, P_3, P_5 model is the one that contains the least number of statistically significant parameters. For the reasons given in § 6 the representation for the X component was taken to be P_1, P_3, P_5, and the representation for the Z component was taken to be the P_1, P_3 model.

The results for the P_1 harmonic for both X and Z data are shown for 1–264 h in figures 17 and 18 respectively. Both curves show some rather interesting features approximately one day into the sequence; the X component increases rapidly to about 40 nT. The field values remain at this level for about 10 h before rising further to about 160 nT, before eventually decaying back to

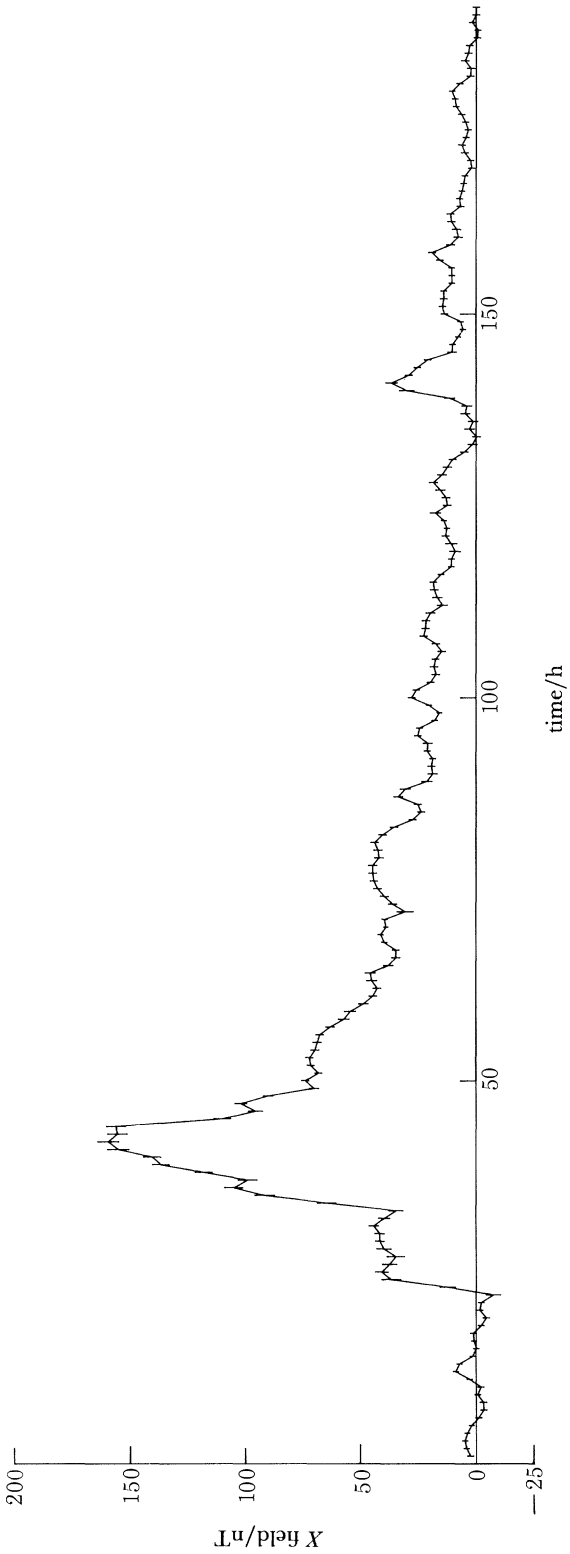

FIGURE 17. P_1 harmonic of the 3 parameter model of the X data for the period beginning 10 February 1969.

PHILOSOPHICAL TRANSACTIONS OF THE ROYAL SOCIETY A MATHEMATICAL, PHYSICAL & ENGINEERING SCIENCES

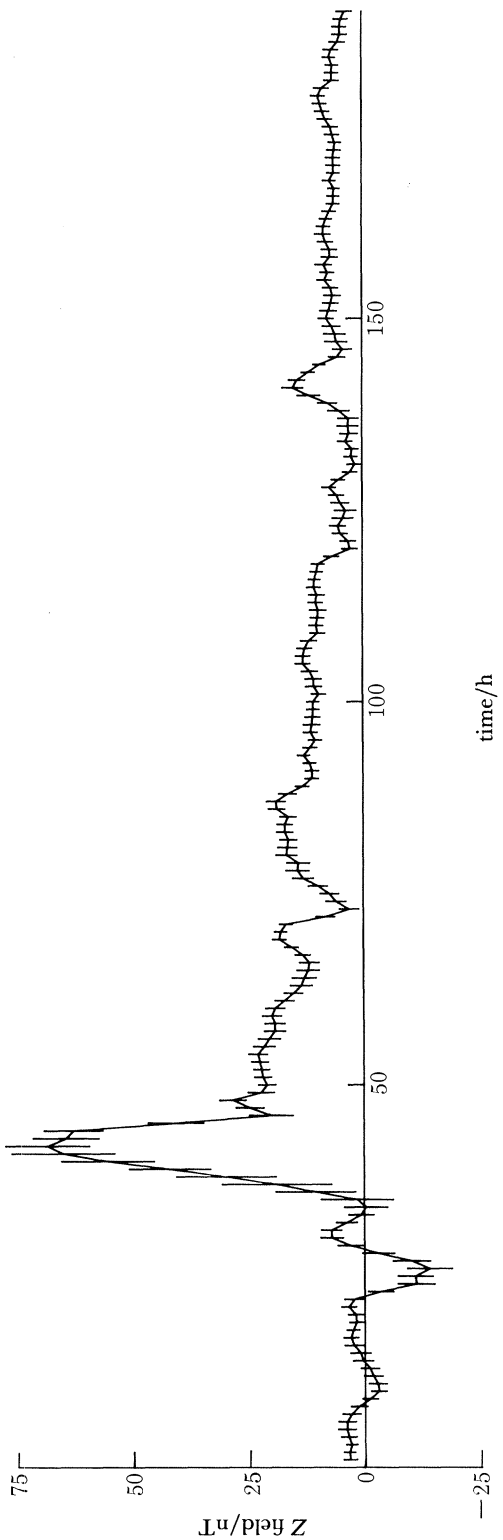

FIGURE 18. P_1 harmonic of the 2 parameter model of the Z data for the period beginning 10 February 1969.

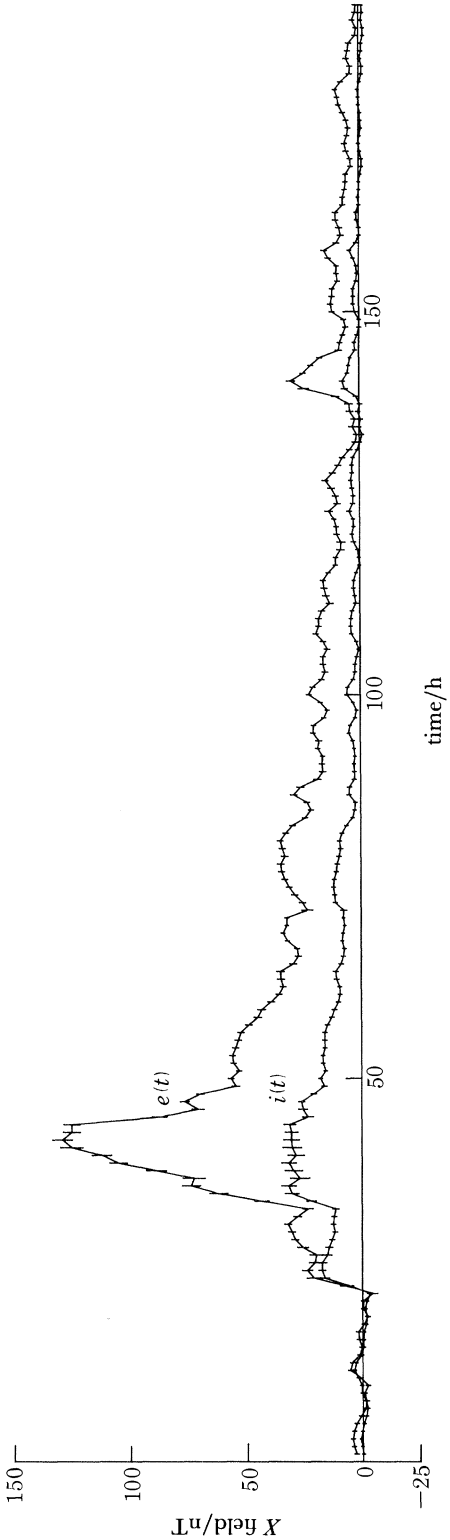

FIGURE 19. The P_1 component of the external and internal parts of the Dst field for the period beginning 10 February 1969.

baseline level. This curious behaviour in the initial stage of the storm is not mirrored in the Z field. Later, during the recovery phase of the storm, both field components show a substorm in the later part of 15 February.

The $e_1(t)$ and $i_1(t)$ fields are displayed in figure 19. Both the external and internal fields level off one day into the sequence, and about 10 h later continue their initial rise to the maximum field variation. The field values during the recovery phase approach the baseline approximately 130 h into the sequence. After this point it appears that a further substorm occurs during the second half of 15 February. This disturbance is of small amplitude and only serves to slightly prolong the recovery phase. It may be noted that no residual daily variation appears in the curves of figures 17–19.

5.5. *The storm of* 8 *March* 1970

For this storm the entry was found to be very poorly defined. In fact, the first 8 days of the month were very disturbed. *I.A.G.A. Bulletin* 32*a* (1970) lists an s.s.c. during 5 March, and Sugiura & Poros (1971) indicate that the early part of the month was disturbed. For these reasons, the data sequence that was chosen for detailed study covers the period from the 6–25 March.

Initially, it was hoped to estimate the baseline with data from before the storm commencement at the beginning of March, however this proved to be unrealistic because of the significantly disturbed field values during this period. After careful consideration and a close inspection of the data and of graphs of equatorial Dst published by Sugiura & Poros, the baseline value for each site dataset was chosen to be the arithmetic mean field value of 24 and 25 March, i.e. 433–480 h inclusive of the record. At that period of the storm it was found that the field had recovered to its undisturbed state.

The daily variation was calculated from the last 10 days of the record, i.e. the period from 16 to 25 March inclusive. Only days containing unbroken data were used, and unless at least 7 days during this period were available for estimating S, the site was removed from the storm analysis. A maximum of 64 observatory records of both X and Z data were included in the analysis.

Figure 20 displays the X magnetic field component measured at Moca, and figure 21 shows the Z component at Wien–Kobenzl. It can be seen that the recovery is steady, and the baseline estimate appears quite realistic. The last 10 days of the sequence are reasonably quiet and provide a good estimate of S. An inspection of the graphs before and after treatment, and the associated power spectra, confirms this. Just before the end of 8 March, the Z field shown in figure 21 shows a sharp dip lasting for approximately 1 h. This feature is rather curious, some site records show it to be rather more pronounced, while others do not show it at all. Noticeable on both diagrams is the disturbed nature of the field before the storm commencement.

After a careful appraisal of the F statistics (Marshall 1980), a P_1, P_3, P_5 representation was adopted for the X data, and a P_1, P_3 representation for Z. The results of the field separation for this storm are based on these models.

It was found that of all the harmonics, P_1 is by far the best defined. Figure 22 shows the total variation field, e_1+i_1. It can be seen that the pre-storm field is significantly disturbed, but the recovery phase is fairly regular with a smooth approach to the baseline value some 300 h or so after the storm onset. Approximately 270 h or so into the record, the X field dips briefly to zero. This dip is also shown in the graph of e_1-2i_1 displayed in figure 23. The pre-storm state, as for

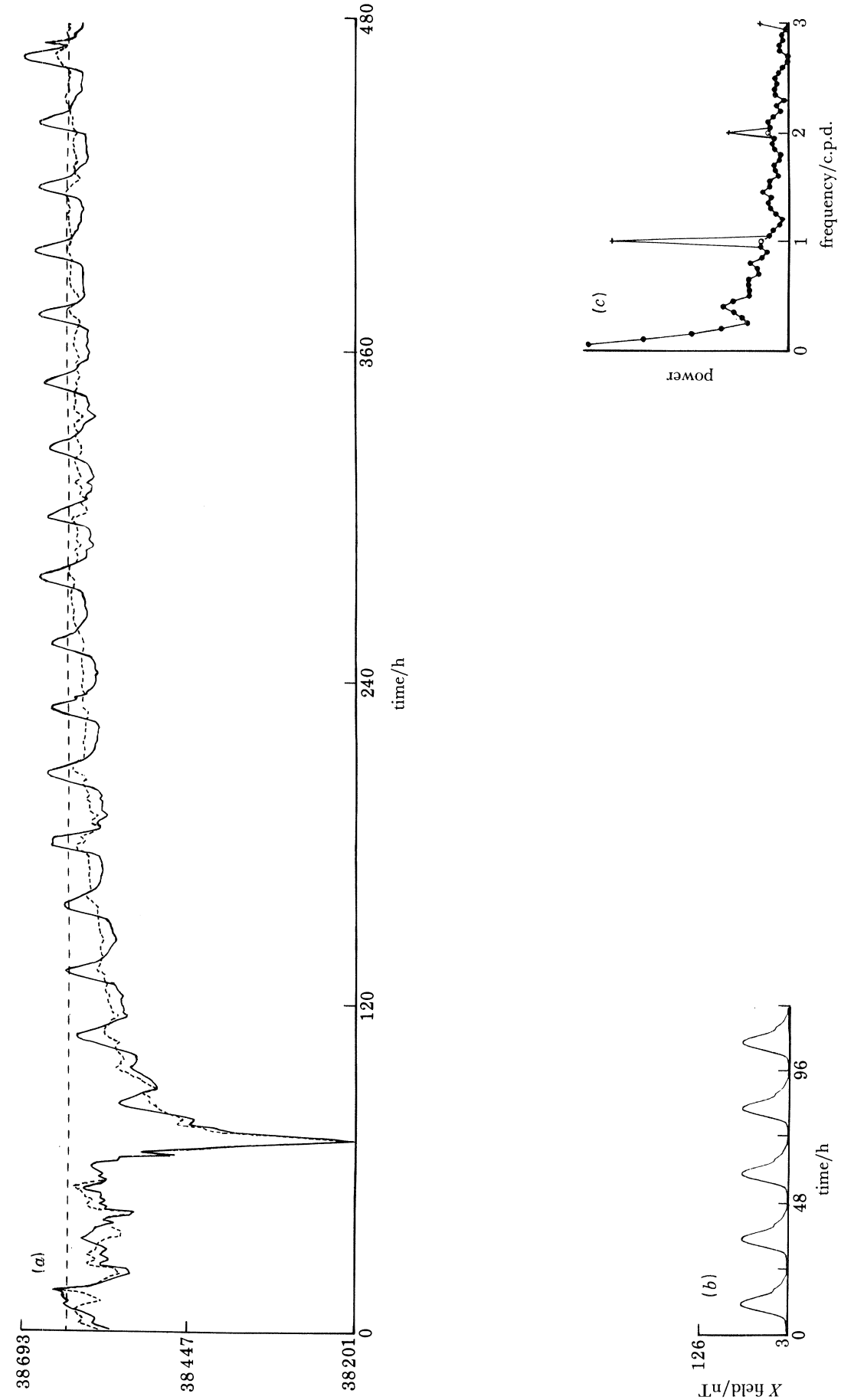

FIGURE 20. Magnetic storm of March 1970. (*a*) Comparison of smoothed (broken line) data to raw data for the *X* field component of Moca. (*b*) The removed periodic component (shown at the same scale as (*a*)). (*c*) The power spectra of the smoothed and raw data.

PHILOSOPHICAL TRANSACTIONS OF THE ROYAL SOCIETY A MATHEMATICAL, PHYSICAL & ENGINEERING SCIENCES

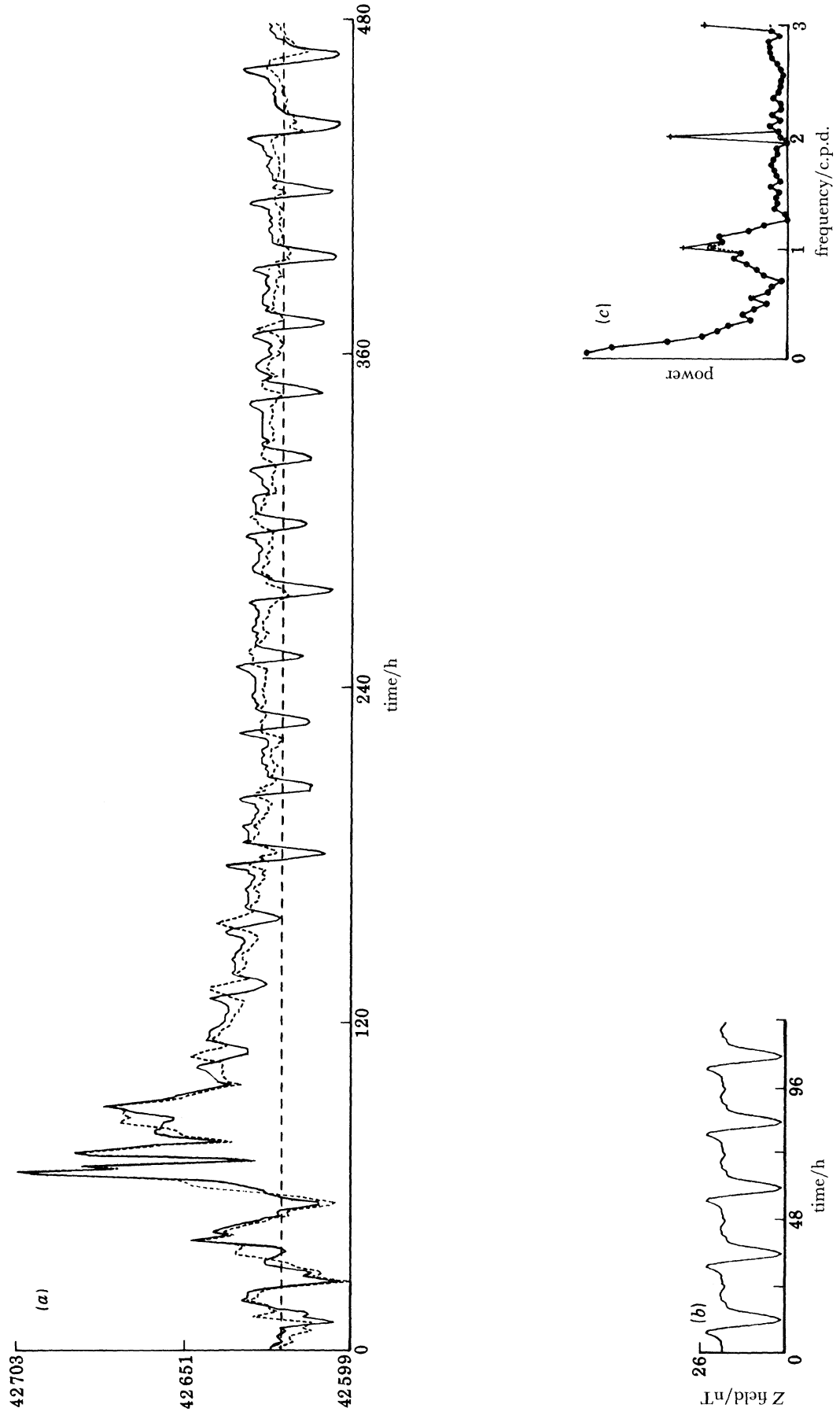

FIGURE 21. Same as figure 20 except that the Z field component measured at Wien–Kobenzl is shown.

PHILOSOPHICAL TRANSACTIONS OF THE ROYAL SOCIETY A MATHEMATICAL, PHYSICAL & ENGINEERING SCIENCES

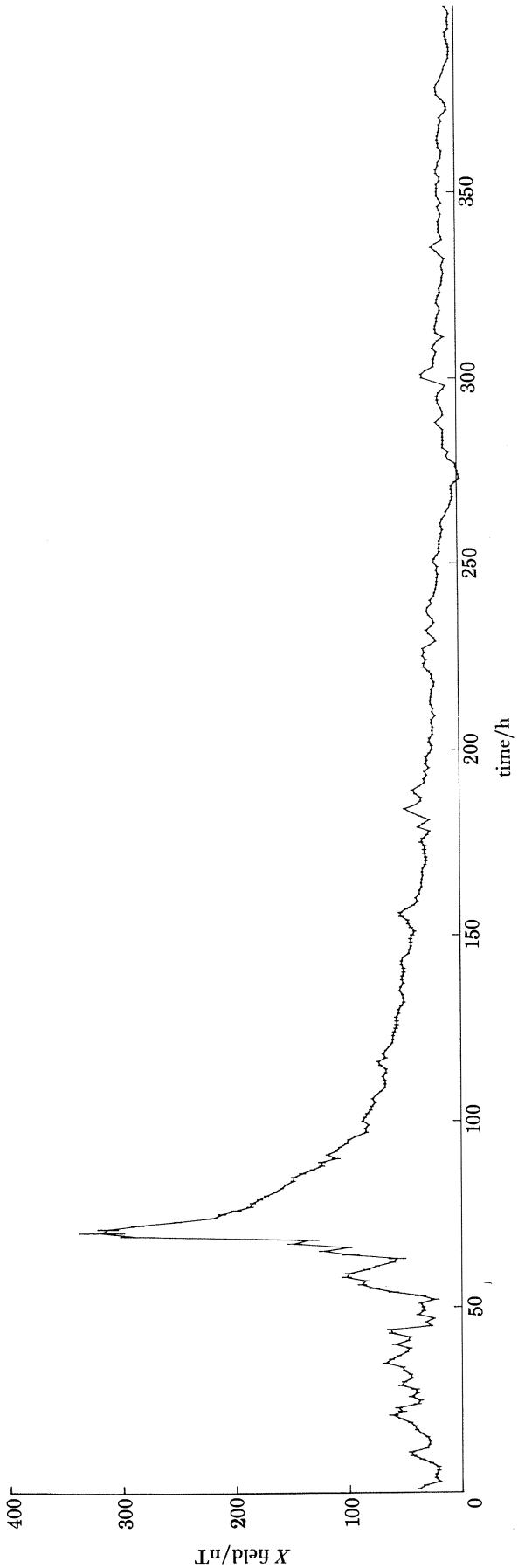

FIGURE 22. P_1 harmonic of the 3 parameter model of the X data for the period beginning 6 March 1970.

PHILOSOPHICAL TRANSACTIONS OF THE ROYAL SOCIETY A MATHEMATICAL, PHYSICAL & ENGINEERING SCIENCES

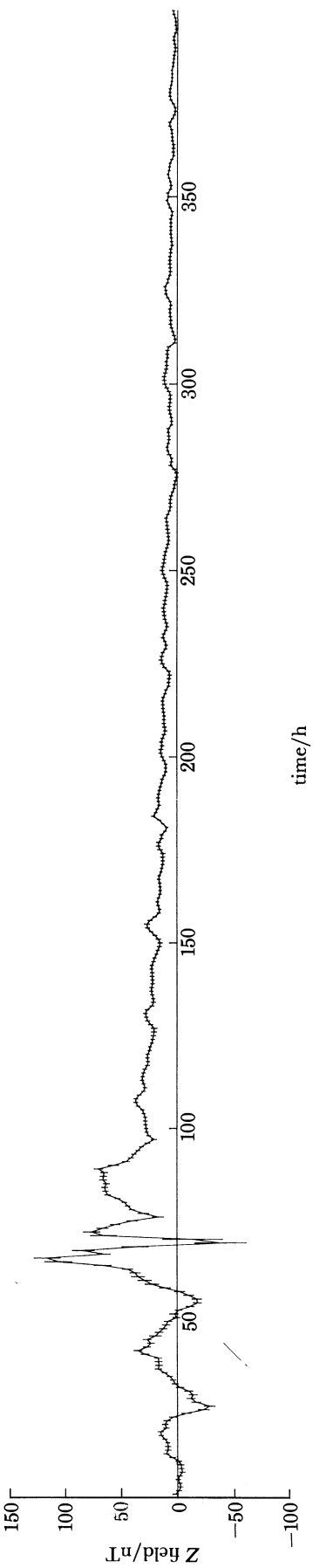

FIGURE 23. P_1 harmonic of the 2 parameter model of the Z data for the period beginning 6 March 1970.

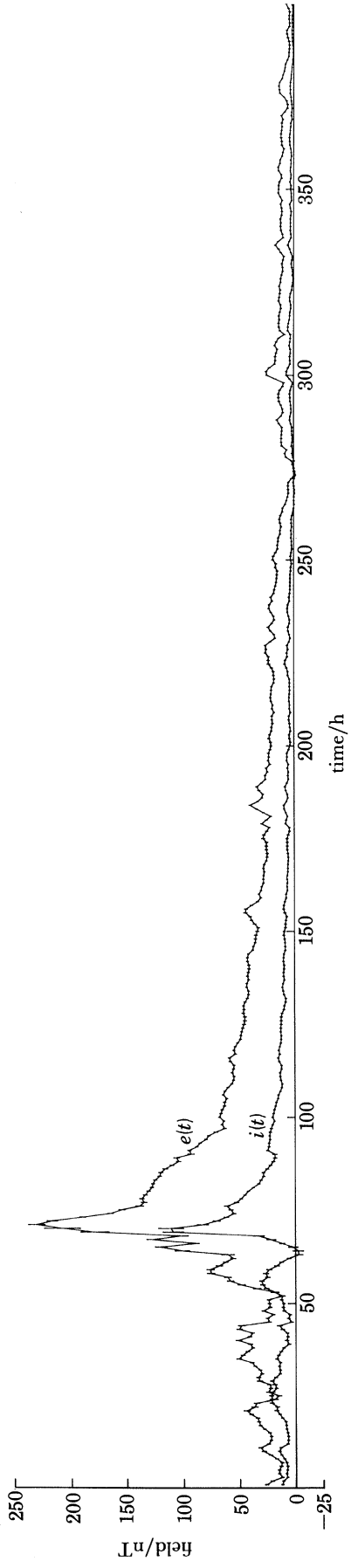

FIGURE 24. The P_1 component of the external and internal parts of the Dst field for the period beginning 6 March 1970 storm.

PHILOSOPHICAL TRANSACTIONS OF THE ROYAL SOCIETY A MATHEMATICAL, PHYSICAL & ENGINEERING SCIENCES

the X field, is very disturbed and unsuitable for baseline estimation. The smooth decay towards the baseline value during the recovery phase is apparent.

The separated $e_1(t)$ and $i_1(t)$ fields can be seen in figure 24. Clearly this storm is the largest of the set analysed here. The maximum external field value is approximately 230 nT, and the maximum internal field about 115 nT. Because of the disturbance at storm commencement as mentioned above, a classical initial phase for the storm cannot be easily discerned. However, the recovery phase is regular and fairly smooth, remaining distinct for up to 14 days after the storm commencement. Physically, this is important for the induced currents associated with these longer period variations penetrate deeper into the mantle, and thus provide information about the conductivity at these depths. Figures 22–24 show no obvious periodic S variation remaining, and confirm that the choice of baseline is physically realistic.

5.6. *The storm of* 16 *August* 1970

For this, the last of the storms analysed here, hourly magnetic field values for the period 10–29 August were used. The storm entry is very clear and the 6 day period before the commencement is free from any notable disturbances. The observatory baseline value was taken to be the arithmetic mean field value during 14 and 15 August, i.e. 97—144 h inclusive. The observatory record was not used if more than 12 of these values were missing.

Estimates of the daily variation, S, for each site were calculated with data from the 10–15, 24 and 29 August. Only days containing unbroken data were used, and for each site record at least 5 of these days were required to estimate S, otherwise the record was removed from the analysis. A maximum of 70 records of X data, and 67 records of Z were ultimately available for analysis.

The X field component at Aquila (figure 25) illustrates the comparatively quiet state of the field during the period 10–15 August. The recovery period lasts about 6 days, and is followed by a few rather disturbed days, which were not used to estimate S. The Z field at San Fernando (figure 26) exhibits the same features.

It was found that the Z data is described with the least number of statistically significant parameters by a P_1, P_3 model. However, the F statistics of the X data, fail to indicate a model that fits the data as well as the initial P_1, P_3, P_5, P_7 test representation. For the reasons given in § 6, the P_1, P_3, P_5 model was used to represent the X field variations. Figures 27 and 28 display the first harmonic for the X and Z fields from 25–320 h. In both diagrams it can be seen that the state of the field before the onset of the storm is undisturbed and stable. An interesting feature that is shown is the second peak during 18 August. This peak is particularly noticeable in the Z field where the peak is almost as high as the field values at the start of the storm. The corresponding peak in the X field is by no means as well pronounced.

The separated fields are shown in figure 29 for the period 15–24 August. The storm commencement is marked by a rapid decrease in both $e_1(t)$ and $i_1(t)$ followed, a few hours later, by a rapid increase in field values. The external field reaches approximately 115 nT and the internal field approximately 75 nT. During the recovery phase, the peak occurring on 18 August appears in the external field but is very poorly displayed in the internal response field. The recovery phase generally appears fairly smooth and physically realistic until 22–23 August. For these days the external field lies between 5 and 20 nT, whereas the internal field is only of the order of a few nanotesla, and for some of the time is negative. This behaviour raises questions about the reliability of the baseline, though the period from which the baseline was calculated appears to

PHILOSOPHICAL TRANSACTIONS OF THE ROYAL SOCIETY A MATHEMATICAL, PHYSICAL & ENGINEERING SCIENCES

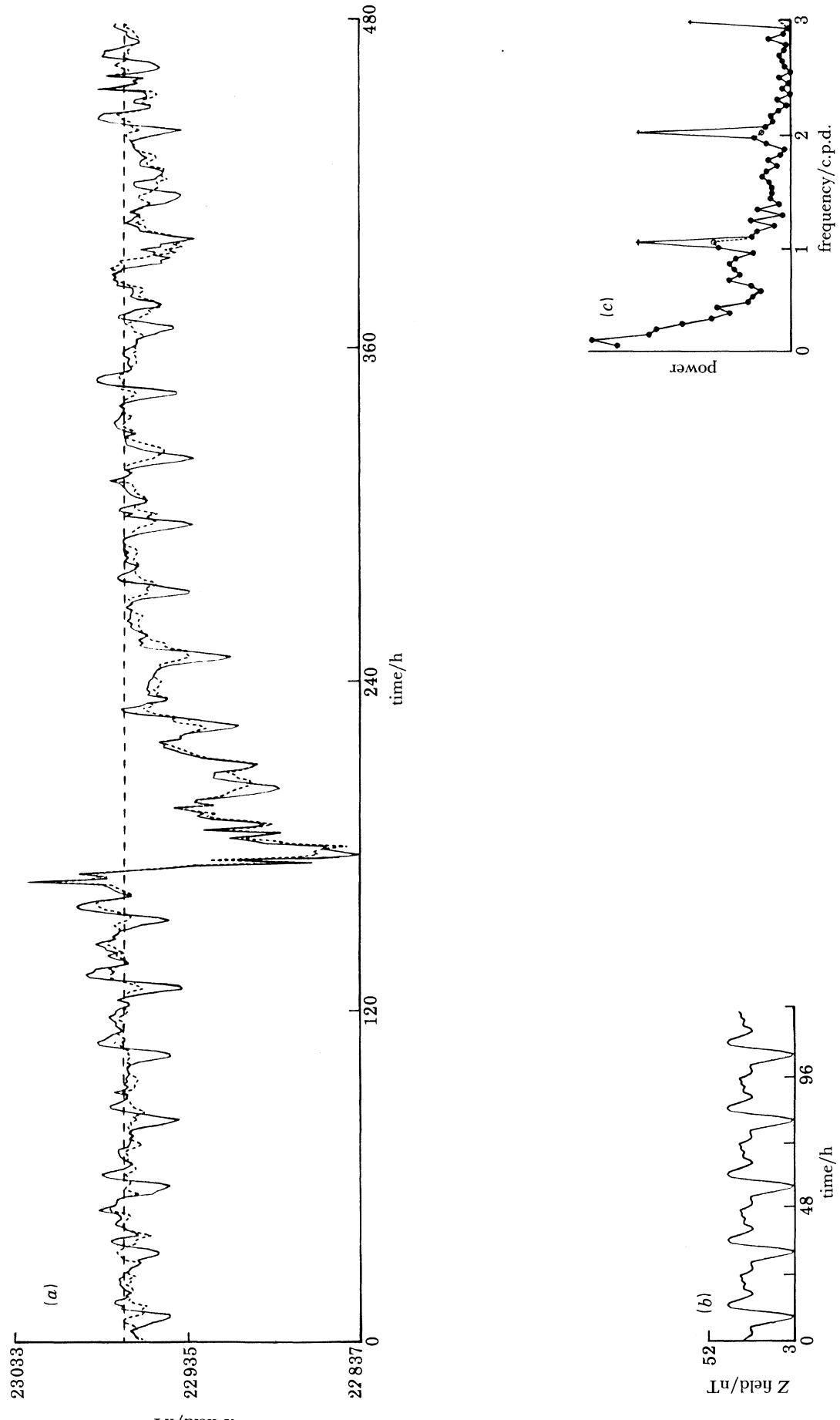

FIGURE 25. Magnetic storm of August 1970. (*a*) Comparison of smoothed (broken line) data to raw data for the *X* field component at Aquila. (*b*) The removed periodic component (shown to the same scale as (*a*)). (*c*) The power spectra of the smoothed and raw data.

PHILOSOPHICAL TRANSACTIONS OF THE ROYAL SOCIETY A MATHEMATICAL, PHYSICAL & ENGINEERING SCIENCES

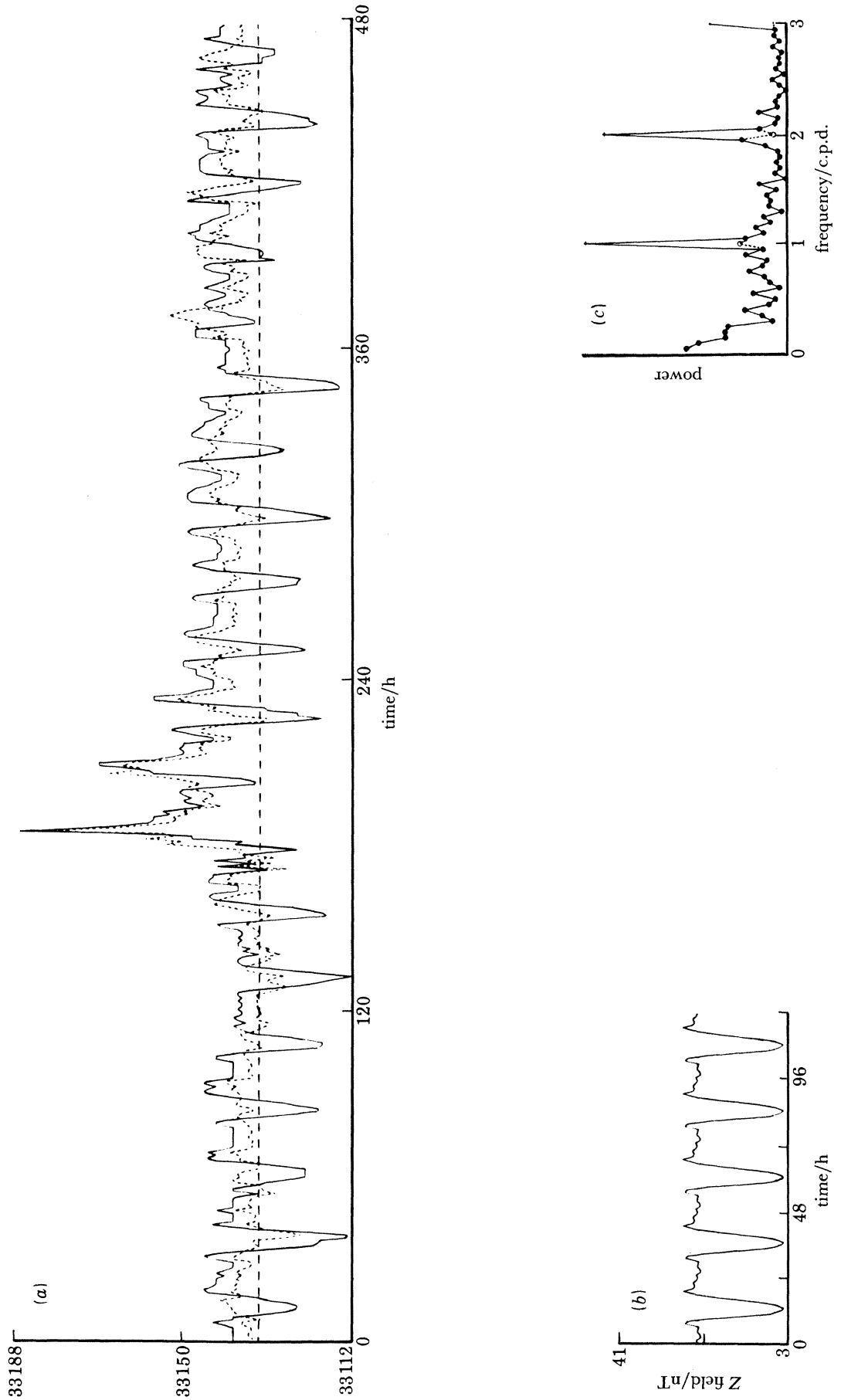

FIGURE 26. Same as figure 25 except that the Z field component at San Fernando is shown.

PHILOSOPHICAL TRANSACTIONS OF THE ROYAL SOCIETY A MATHEMATICAL, PHYSICAL & ENGINEERING SCIENCES

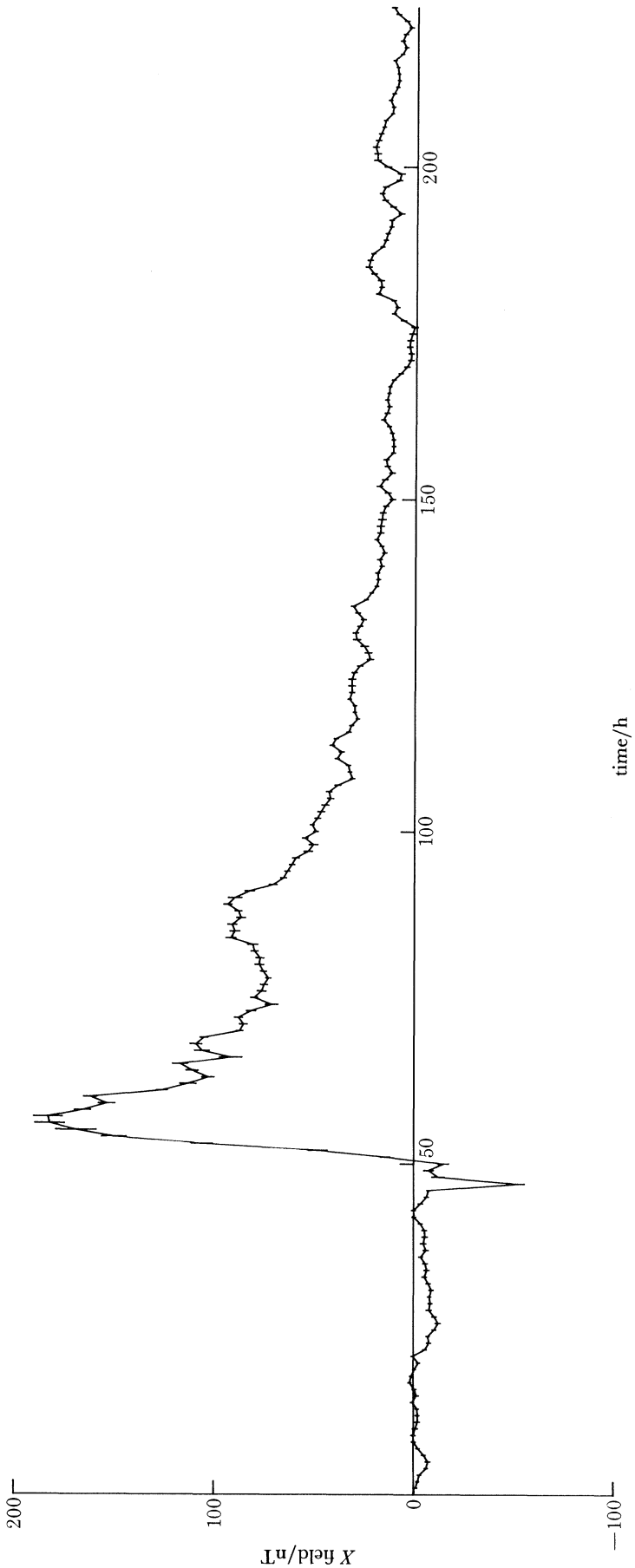

FIGURE 27. P_1 harmonic of the 3 parameter model of the X data for the period beginning 15 August 1970.

PHILOSOPHICAL TRANSACTIONS OF THE ROYAL SOCIETY A MATHEMATICAL, PHYSICAL & ENGINEERING SCIENCES

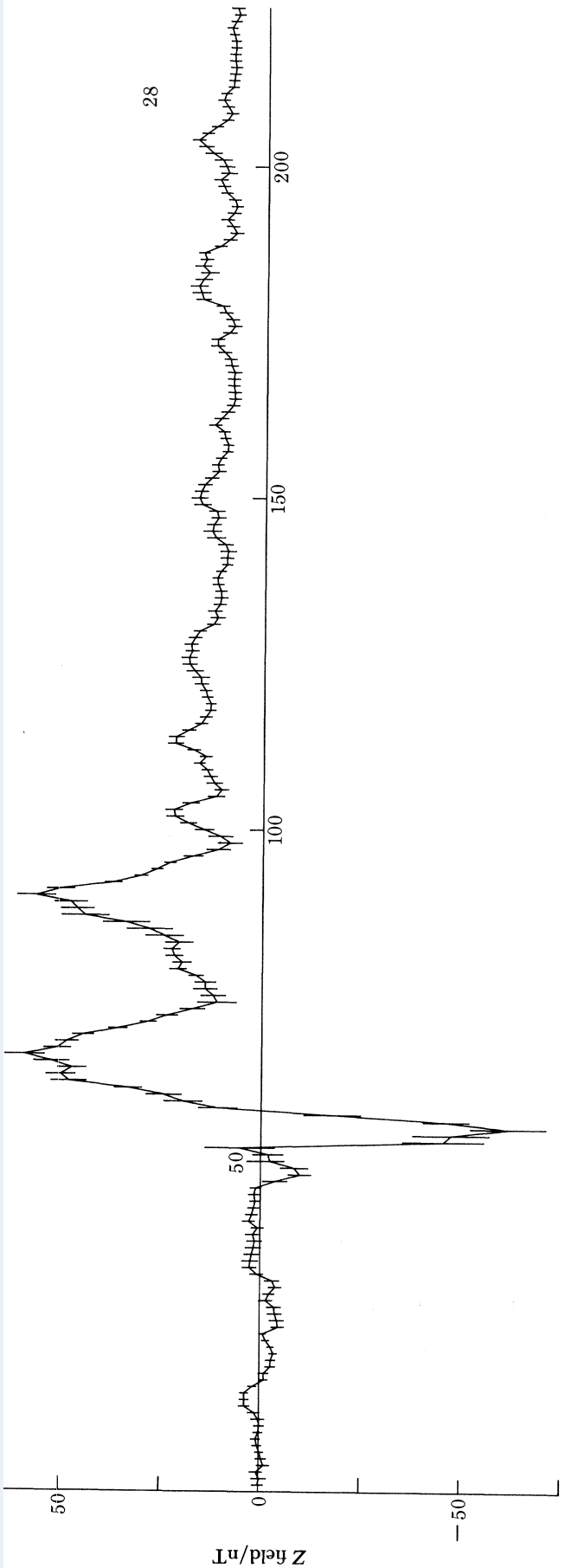

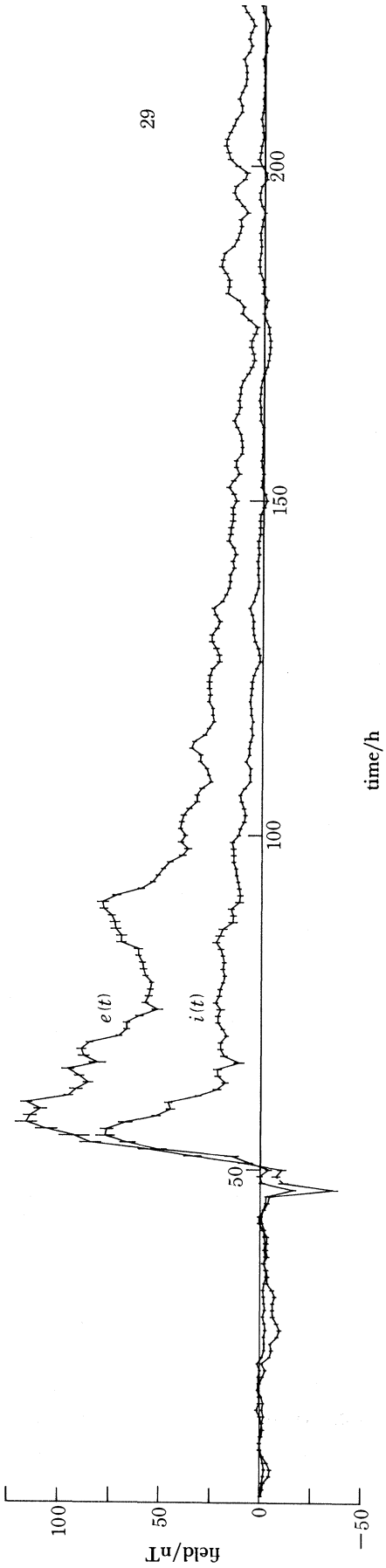

FIGURE 28. P_1 harmonic of the 2 parameter model of the Z data for the period beginning 15 August 1970.

FIGURE 29. The P_1 component of the external and internal parts of the Dst field for the period beginning 15 August 1970.

PHILOSOPHICAL TRANSACTIONS OF THE ROYAL SOCIETY A MATHEMATICAL, PHYSICAL & ENGINEERING SCIENCES

represent well the undisturbed, normal state of the field and is well shown in the graphs of equatorial Dst by Sugiura & Poros (1971).

An inspection of figures 27–29 and of the equivalent results for the single component, P_1, model, fails to show any distinct 24 h variation in the middle and latter parts of the recovery phase. The removal of the daily variation appears therefore to be satisfactory, and supports the conclusion that figures 27–29 are essentially correct in their presentation of the field variations.

6. Assessment of results

In determining the appropriate harmonic representation of both the X and Z magnetic field components during the recovery phase of each of the storms studied here, useful guidance has been afforded by using the F statistics. The results for the X magnetic field show that for three of the storms analysed (§§ 5.1, 5.2, and 5.3), the model with the least number of statistically significant parameters is the P_1, P_3, P_5 representation. For the remaining 3 storms no model can be found, with less parameters, that fits the data as well, in a statistical sense, as the P_1, P_3, P_5, P_7 model.

The results for the Z magnetic field show that for 3 of the storms (§§ 5.1, 5.2, and 5.4), the model with the least number of statistically significant parameters is the P_1, P_3 representation, whereas for the remaining storms it is the P_1, P_3, P_5 model.

It is interesting to note that the recovery phase of Dst variations appears to be rather better defined during the quiet part of the solar cycle, in the sense that both X and Z magnetic field components tend to require fewer harmonics to represent the global field variations. The coefficient of the first, P_1, harmonic is dominant, though P_3, sometimes P_5 or even higher order harmonics, although much smaller, are statistically important.

During the active part of the solar cycle, more parameters may be required because field variations of high frequency (over 5 c.p.d.) occur more frequently than during the quiet part, and are of greater amplitude. In fact the higher F values are distributed in groups (Marshall 1980), possibly because they represent high frequency variations lasting for only a few hours at a time. The induced currents at these high frequencies do not penetrate more than a few hundred kilometres into the mantle and are much affected by lateral inhomogeneities in electrical conductivity. This means that a model consisting of a small number of Legendre polynomials is inadequate to describe the field variations when dominated by high frequency variations.

For purposes of determining global field variations conforming to a spherically symmetric conductivity profile, the analysis of Dst during the quiet part of the solar cycle may best indicate the number of parameters that are necessary. Consecutive models analysing the X field variations produce a stable estimate of the first harmonic component. That is the P_1 component of, for example, the P_1, P_3, P_5 and the P_1, P_3, P_5, P_7 models are very similar. Any variation that does occur can be measured in terms of a few nanotesla at most, and in practice the choice of the representation for the X data does not significantly affect the final estimates of $e_1(t)+i_1(t)$.

The stability of the P_1 estimates is not found for the Z field variations. All the storms analysed here display a very similar P_1 field for the P_1 harmonic only, and the P_1, P_3 models. When more parameters are added, the model begins to break down and the P_1 term becomes physically unrealistic. For instance, during the initial stages of the storm e_1-2i_1 has far higher values than can be realistically expected. Furthermore, the estimated values of the other parameters also

increase and approach the values of the P_1 harmonic terms. The choice of the representation for the Z data is important and may significantly affect the final estimates of $e_1(t)$ and $i_1(t)$.

It should be noted that the expansion for the Z field is in terms of an orthogonal set of functions. However, each component is not independent since the process used here is effectively a least squares estimate that does not involve integration over the sphere. A possible explanation for the problems that occur with the Z field analysis is available. For the first harmonic term at co-latitude θ,

$$\left.\begin{aligned} Z_1(t,\theta) &= \{e_1(t) - 2i_1(t)\}\cos\theta, \\ X_1(t,\theta) &= -\{e_1(t) + i_1(t)\}\sin\theta. \end{aligned}\right\} \tag{6.1}$$

At zero frequency, the response ratio, $S_1(\omega)$, must be zero, since a static magnetic field cannot induce any magnetic field in a conductor with vacuum permeability. The response ratio is given by the formula $S_1(\omega) = I_1(\omega)/E_1(\omega)$, where $I_1(\omega)$ and $E_1(\omega)$ are respectively the Fourier transforms of $i_1(t)$ and $e_1(t)$. As the frequency tends to infinity, any conducting sphere tends to behave as a perfectly conducting sphere for which $S_1(\omega) = 0.5$. In the time domain we can expect $i_1(t)/e_1(t)$ to range from zero, for variations that change slowly with time, to 0.5 for rapid variations. Clearly $e_1(t) - 2i_1(t)$ is far smaller than $e_1(t) + i_1(t)$, as is confirmed by examination of the results of the storm analyses. There is a further complication in that the data is drawn from observatories within $\pm 55°$ of the geomagnetic equator. Equations (6.1) show that in this range the X field variations attain their maximum values, whereas the Z field variations reach their minimum. This inherent geometrical factor ensures that the Z field Dst variations are much smaller than those of the X field.

Models containing more than 2 harmonics may over parameterize the Z variations, which may at times be difficult to distinguish from background noise. The X variation is much larger in amplitude and thus relatively free from contamination by noise, so that more parameters may be used. It is clear that the F statistic test should not be regarded as a rigid rule that determines the representation to be taken, but that the nature of the data must also be taken into account, Furthermore, the F test depends on the assumption that the errors, γ_j, form a normal distribution with zero mean. This assumption is a realistic one, though in practice it should be realised that it is only a good approximation and not exact. For these reasons it is advisable to use the F statistic as a guide only, and in this case it was decided to adopt the P_1, P_3, P_5 model to represent the X Dst variations, and the P_1, P_3 combination to represent the Z Dst field.

An interesting feature that occurs in all of the storms presented here is that during the first few hours of the disturbance, the internal field initially rises very rapidly in response to the external field increase, but before the external field reaches its peak, the internal field has checked its rise. Similar effects can be seen in the previous analyses by Chapman & Price (1930), and Anderssen *et al.* (1970). The reasons for this behaviour are not immediately apparent, but may be due to the mutual interaction of the induced currents themselves at different depths within the mantle.

Anderssen *et al.* analysed the storm of 1958. Their analysis covered 35 h storm time starting from storm commencement, and the baseline was taken to be the field value at the hour immediately before the s.s.c. They found that the X data was represented by the least number of statistically significant parameters by a P_1, P_3 model. For the Z data, no model containing less parameters than their original P_1, P_3, P_5, P_7 test model could be found to adequately represent the data. It is possible that the choice of baseline proved to be inadequate and undermined the statistical testing,

PHILOSOPHICAL TRANSACTIONS OF THE ROYAL SOCIETY A MATHEMATICAL, PHYSICAL & ENGINEERING SCIENCES

or simply that their analysis was at the beginning of the storm when high frequency variations predominate. They also found very little difference in the results obtained by using data before S was removed from it, or after. It is found in the present work, that failure to remove the daily variation from the data leads to a residual periodic variation appearing in $e_1(t)$ and $i_1(t)$. This leads to an increase in the standard errors and a weakening of the statistical testing.

In conclusion, it is found that data preparation is of paramount importance. Records should first be checked for any possible recording errors such as observatory baseline changes. Close attention has to be paid to the efficiency of the method of smoothing out the daily variation, and the reliability of the baseline estimates. Although the methods of removing S, and estimating the baseline as used here are not perfect, they are physically realistic, relatively simple to apply, and produce physically acceptable results. Finally, analysis of as much of the recovery phase as possible is strongly recommended. The disturbance of March 1970 shows well defined external and internal field values for up to 14 days after the storm commencement, it is these longer period variations that are so important for determining the deeper conductivity within the mantle.

One of us (R.T.M.) is grateful to S.R.C. (now S.E.R.C.) for financial support while this work was being done at the University of Exeter. We have both benefitted from discussions with Dr R. S. Anderssen, and are grateful to him for his interest in our work.

References

Anderssen, R. S. & Seneta, E. 1969 *J. geophys. Res.* **74**, 2768–2773.
Anderssen, R. S., Doyle, H. A., Petersons, H. F. & Seneta, E. 1970 *J. geophys. Res.* **75**, 2569–2577.
Anderssen, R. S. & Seneta, E. 1971 *Math. Geol.* **3**, 157–170.
Bailey, R. C. 1970 *Proc. R. Soc. Lond.* A **315**, 185–194.
Birkeland, K. 1908 *The Norwegian aurora Polaris expedition*, 1902–1908, 1st edn, pp. 39–315. Christiania, Norway: H. Aschebourg & Co.
Campbell, W. H. & Matsushita, S. (eds) 1967 *Physics of geomagnetic phenomena*, 2 vols. New York: Academic Press.
Chapman, S. 1918*a* *Proc. R. Soc. Lond.* A **95**, 61–83.
Chapman, S. 1918*b* *Mon. Not R. astr. Soc.* **79**, 70–83.
Chapman, S. & Bartels, J. 1940 *Geomagnetism.* Oxford: The Clarendon Press.
Chapman, S. & Price, A. T. 1930 *Phil. Trans. R. Soc. Lond.* A **229**, 427–460.
Devane, J. F. 1977 *Acta Geod., Geophys. et Montanist. Acad. Sci Hung.* **13**, 369–375.
Jady, R. J., Marshall, R. T. & Morgan, K. 1979 *Physics Earth planet. Inter.* **20**, 6–10.
Lahiri, B. N. & Price, A. T. 1939 *Phil. Trans. R. Soc. Lond.* A **237**, 509–540.
Malin, S. R. C. 1973 *Phil. Trans. R. Soc. Lond.* A **274**, 551–594.
Marshall, R. T. 1980 *Geomagnetic storm-time variations and the determination of Upper Mantle conductivity*, Ph.D. thesis, University of Exeter.
Matsushita, S. 1964 In *Research in geophysics* (ed. H. Odishaw), vol. 1, pp. 455–483. Cambridge, Massachusetts: M.I.T. Press.
Mood, A. M. & Graybill, F. A. 1963 Introduction to the theory of statistics, 2nd edn. New York: McGraw-Hill Book Co.
Parker, R. L. 1972 *Geophys. Jl R. astr. Soc.* **29**, 123–138.
Parker, R. L. 1977 *Geophys. Jl R. astr. Soc.* **49**, 513–547.
Parker, R. L. 1980 *J. geophys. Res.* **85**, 4421–4428.
Parker, R. L. & Whaler, K. A. 1981 *J. geophys. Res.* **86**, 9574–9584.
Rikitake, T. 1966 *Electromagnetism and the Earth's interior, Developments in solid Earth geophysics*, vol. 2. Amsterdam: Elsevier.
Rikitake, T. & Sato, S. 1957 *Bull. Earthq. Res. Inst. Tokyo Univ.* **35**, 7.
Schmucker, U. 1970 *J. Geomagn. Geoelectr., Kyoto* **22**, 9–33.
Schmucker, U. 1970 *Bull. Scripps Instn Oceanogr.* **13**.
Schmucker, U. 1977 *Acta geod., geophys. et Montanist. Acad. Sci. Hung.* **13**, 1–3.
Sugiura, M. & Poros, D. J. 1971 *Hourly values of Equatorial Dst for the years* 1957–1970, Report of Goddard Space Flight Center, Greenbelt, Maryland, U.S.A.
Weidelt, P. 1972 *Z. Geophys.* **38**, 257–289.

PHILOSOPHICAL TRANSACTIONS OF THE ROYAL SOCIETY A MATHEMATICAL, PHYSICAL & ENGINEERING SCIENCES